博士論文

# **Pathogenesis of EVI-1 Overexpressing Acute Myeloid Leukemia**

（**EVI-1** 高発現白血病の病態解明）

水野秀明

博士論文

# Pathogenesis of EVI-1 Overexpressing Acute Myeloid Leukemia

（**EVI-1** 高発現白血病の病態解明）

所属　東京大学大学院医学系研究科内科学専攻　血液・腫瘍病態学
指導教員　　黒川　峰夫　教授

申請者　　水野　秀明

Contents

【**Abstract**】

Acute myeloid leukemia (AML) is a heterogeneous disease with variable prognosis depending on genetic abnormalities. AML with Evi1 overexpression (Evi1$^{high}$ leukemia) due to chromosomal abnormalities or other transcriptional dysregulations is one of the subgroups with the poorest prognosis in the disease. Although a variety of mechanisms of how Evi1 contributes to leukemia progression have been reported, effective therapeutic targets of Evi$^{high}$ leukemia have not been identified. In this study, I thoroughly explored gene expression profiles in Evi1-overexpressing leukemia cells. I identified two novel targets regulated by Evi1, p57$^{KIP2}$ and Fbp1 through analyzing RNA-seq data of an Evi1-overexpressing mouse leukemia model. While p57$^{KIP2}$ was downregulated upon leukemic transformation, Fbp1 expression was further increased at later time points. Through investigating a role of Fbp1 in Evi1 leukemia cells, I showed the importance of altered glucose metabolism in Evi1 leukemia cells *in vivo*. Collectively, these findings provide insights on molecular pathogenesis and new promising therapeutic targets for Evi1$^{high}$ leukemia.

【Introduction】

Acute myeloid leukemia (AML) is one of the common hematologic malignancies characterized by differentiation arrest and a clonal expansion of immature hematopoietic progenitor or stem cells mainly in bone marrow and peripheral blood [1]. Its prognosis is highly heterogeneous depending on its molecular profiles. A number of genetic abnormalities and accompanying transcriptomic characteristics are related to poor prognostic AML, which is resistant to standard chemotherapy. Deregulated expression of ecotropic viral integration site 1 (Evi1) occurs in approximately 10% of AML, which is encoded by the *MECOM* gene located on human chromosome 3q26 [2-9]. In World Health Organization classification, acute myeloid leukemia with inv(3)(q21q26.2) or t(3;3)(q21;q26.2) is categorized as a distinct disease entity with poor prognosis and related to thrombocythemia and dysplastic changes of myeloid cell lineage and megakaryocytes. These chromosomal changes involve the MECOM gene locus and result in high Evi1 expression in a GATA2 enhancer-dependent manner [2, 10, 11]. Evi1 is a nuclear transcription factor indispensable for proliferation and stemness of normal hematopoietic stem cells (HSCs), whereas it also contributes to leukemogenesis by multiple mechanisms such as suppressing transforming growth factor-β (TGF-β) signaling, inhibiting c-Jun N-terminal kinase, activating activator protein-1 (AP-1), upregulating mammalian target of rapamycin (mTOR) signaling pathway through phosphatase and tensin homologue deleted from chromosome 10 (PTEN) repression, and inducing PU.1 mediated myeloid skewing through Spi1 upregulation [13-19]. On the other hand, several other studies showed that Evi1 overexpression in hematopoietic cell lines and mouse hematopoietic progenitor cells induced anti-proliferative effects, cell cycle arrest in G0/G1 phase and spontaneous increase of apoptosis [20-23]. This effect is partially explained by elevated expression of cell-cycle dependent kinase inhibitor genes, such as *Cdkn1b*, *Cdkn1c*, and *Cdkn2c* [20]. These apparently contradictory effects may be due to the difference between short- and long-term effects of Evi1 expression on cellular phenotypes; although Evi1 transiently promotes cellular quiescence through upregulating stemness-related genes, it positively affects long-term cell survival and proliferation.

Recently metabolome analysis of Evi1-overexpressing leukemia cells revealed that Evi1 induces metabolic vulnerability due to dependence on creatine kinase pathway [24, 25]. Transcriptome analysis of Evi1-transduced mouse bone marrow cells suggested alteration of some important metabolic pathways such as glycolysis, pentose phosphate pathway, and purine and pyrimidine metabolism. Moreover, metabolome analysis of Evi1-transduced mouse bone marrow lineage negative cells revealed that steady state levels of 82 small metabolites such as deoxynucleotide triphosphates were significantly changed compared to control cells [24]. Metabolic characteristics of leukemia stem cells and chemotherapy resistance were also reported recently. Metabolome analysis of human primary AML cells demonstrated that leukemia stem cells (LSCs) defined as low reactive oxygen species (ROS) cells showed increased amino acid levels compared to high ROS non-LSCs and that inhibition of amino acids uptake efficiently decreased LSCs [62]. In another report, AML cells collected from relapsed AML patients showed higher oxidative phosphorylation activity compared with primary AML cells [50]. On the other hand, aerobic glycolysis, also known as Warburg effect, is one of main metabolic characteristics of malignant cells, in which glucose tends to be converted to lactate irrelevant to oxygen availability, which results in rapid ATP synthesis to fulfill the ATP demand of rapidly proliferating cancer cells [26, 27]. In line with this idea, proliferation of MLL-AF9-induced AML is more easily compromised by inhibition of glycolysis enzymes than normal hematopoietic stem cells [28]. Since these reports suggest that alterations of metabolic profiles would be the important features and therapeutic targets of specific AML subtypes, a deeper understanding of metabolic profiles alteration of Evi1 high leukemia is required.

In this study, I sought to clarify specific molecular features of AML with high Evi1 expression by using an Evi1-overexpressing leukemia mouse model that had previously been established [5]. RNA-sequencing analysis of Evi1-overexpressing pre- and post-leukemia cells revealed distinct transcriptomic profiles. I found that transcriptomic regulation of $p57^{KIP2}$ and Fbp1 by Evi1 overexpression contributes to the development and progression of leukemia. Furthermore, I showed that Evi1 overexpression-mediated metabolic alteration in which the pentose phosphate pathway and oxidative phosphorylation become more important glucose metabolism pathway. Taken together, these results provide a potential therapeutic target of AML with high Evi1 expression.

【Methods】

**Plasmids**

pMYs-murine Evi-1-internal ribosome entry site (IRES)-green fluorescent protein (GFP) vector was produced by cloning murine Flag-tagged Evi1 cDNA into the multiple cloning site of pMYs-IRES-GFP. pGCDN-p57$^{KIP2}$-KusabiraOrange and pGCDN-p57 mutant-KusabiraOrange was produced by cloning p57 and p57 mutant construct into the multiple cloning site of pGCDN-KusabiraOrange. The p57 mutant lacks a cyclin-dependent kinase inhibitory domain (amino acids 1-80) [52, 53]. The p57 and p57 mutant constructs were kindly provided by Dr. Y. Gotoh (The University of Tokyo, Tokyo, Japan) [29]. To obtain short hairpin RNA for silencing the target *Fbp1*, *G6pd*, *Pgd* and *Rpia* genes, oligonucleotides with BamHI or EcoRI restriction site at its 5' end, 19 bases of sense strand, 9 bases of hairpin loop, 19 bases of antisense strand, 6 bases of terminator, and 6 bases corresponding to a unique MluI restriction site were synthesized. These oligonucleotides were annealed and inserted into the BamHI and EcoRI sites of the RNAi-Ready pSIREN-RetroQ-DsRed Vector or RNAi-Ready pSIREN-puro Vector (Clontech, CA). Target sequences of shRNAs for these genes were selected by using Clontech RNAi Target Sequence Selector (http://bioinfo.clontech.com/rnaidesigner/sirnaSequenceDesignInit.do) and are described separately (Table 1). The shRNA targeting the luciferase gene was used as control. All sequences of inserted site were verified by DNA sequencing.

Table1. shRNA insert oligo sequences.

| oligo name | Sequence |
|---|---|
| sh-*Fbp1*-1 top | GATCCGCCAGGACTCAAGTTCATTGTTCAAGAGACA ATGAACTTGAGTCCTGGTTTTTACGCGTG |
| sh-*Fbp1*-1 btm | AATTCACGCGTAAAAACCAGGACTCAAGTTCATTG TCTCTTGAACAATGAACTTGAGTCCTGGCG |
| sh-*Fbp1*-2 top | GATCCGCTTTGACCCTGCCATCAATTTCAAGAGAAT TGATGGCAGGGTCAAAGTTTTTACGCGTG |
| sh-*Fbp1*-2 btm | AATTCACGCGTAAAAACTTTGACCCTGCCATCAAT TCTCTTGAAATTGATGGCAGGGTCAAAGCG |
| sh-*G6pd*-1 top | GATCCGCGGCAACTAAACTCAGAATTCAAGAGATTC TGAGTTTAGTTGCCGCTTTTTACGCGTG |
| sh-*G6pd*-1 btm | AATTCACGCGTAAAAAGCGGCAACTAAACTCAGAA TCTCTTGAATTCTGAGTTTAGTTGCCGCG |
| sh-*G6pd*-2 top | GATCCACCAGATCTACCGCATTGATTCAAGAGATCA ATGCGGTAGATCTGGTTTTTTACGCGTG |
| sh-*G6pd*-2 btm | AATTCACGCGTAAAAAAACCAGATCTACCGCATTGA TCTCTTGAATCAATGCGGTAGATCTGGTG |
| sh-*Pgd* top | GATCCGCTGGAAGGCAGTAAGAAGTTTCAAGAGAAC TTCTTACTGCCTTCCAGTTTTTACGCGTG |
| sh-*Pgd* btm | AATTCACGCGTAAAAACTGGAAGGCAGTAAGAAGT TCTCTTGAAACTTCTTACTGCCTTCCAGCG |
| sh-*Rpia* top | GATCCGTGGACACAGGCCTTTTCATTTCAAGAGAAT GAAAAGGCCTGTGTCCATTTTTACGCGTG |
| sh-*Rpia* btm | AATTCACGCGTAAAAAATGGACACAGGCCTTTTCAT TCTCTTGAAATGAAAAGGCCTGTGTCCACG |

**Retrovirus production and transduction**

To produce retroviruses, Plat-E packaging cells were transiently transfected with 12µg of each retrovirus vector mixed with 96µl of PEI and 500µl of 150mM NaCl, followed by incubation at 37°C. Culture medium was replaced 12 hours after transfection. The retrovirus-containing supernatant was collected 24 hours after medium change, filtered through 0.45 µm membrane, and added to the culture plate coated with RetroNectin (Takara Bio, Japan). Culture plate was centrifuged at 2000g, 37°C for 4 hours and supernatant was discarded. Cells were seeded onto the virus-binding plate and infected with retroviruses for 48 hours.

**Isolation of murine bone marrow cells**

C57BL/6 mice were sacrificed by cervical dislocation. Femora, tibiae, ilia were excised, cleaned of attached mouse tissue, and stored on ice in PBS. After crushing these bones in PBS, bone marrow cells in supernatant were collected through 70µm EASY strainer™ (Greiner Bio One, Australia), centrifuged at 1500rpm 5 minutes, resuspended in 4ml of cold PBS and carefully layered onto the Histopaque-1077 (Sigma-Aldrich, MO) in a 15ml conical centrifuge tube. After centrifugation at 400g for 30 minutes at room temperature, opaque interface containing mononuclear cells were added into 10ml of PBS, and centrifuged at 250g for 5 minutes.

**Flow cytometry**

Cell sorting and analysis were performed by using FACS AriaIII (BD Biosciences, NJ) and FACS AriaII (BD Biosciences). The data were analyzed using FACSDiva software (BD Biosciences) and FlowJo software (FlowJo LLC, OR). For staining murine cells, The following antibodies were used: APC anti-CD117/c-Kit antibody (BioLegend, CA), PE/Cy7 anti-CD117/c-Kit antibody (BioLegend), PE/Cy7 anti Sca-1 antibody (BioLegend), PerCP/Cy5.5 anti Sca-1 antibody (BioLegend), PE anti CD16/32 antibody (BioLegend), Alexa647 anti CD34 antibody (BioLegend), biotin anti-CD3 antibody (BioLegend), biotin anti-CD4 antibody (BioLegend), biotin anti-CD8 antibody (BioLegend), biotin anti-Gr1 antibody (BioLegend), biotin anti-Mac1 antibody (BioLegend), biotin anti-Ter119 antibody (BioLegend), biotin anti-B220 antibody (BioLegend), biotin anti-CD127 antibody (BioLegend). Biotin conjugated antibodies were used as a lineage marker. To visualize biotin conjugated antibodies, PerCP/Cy5.5 streptavidin (BioLegend) or APC/Cy7 streptavidin (BioLegened) was used. To stain cells, 0.5-1μl of each antibody was added to 100μl of isolated mononucleated cell suspended

PBS with 3% FCS and incubated 30minutes on ice. To detect apoptotic cells, 0.5μl of 20mg/ml 4',6-diamidino-2-phenylindole (DAPI) (Sigma-Aldrich) was added to each sample. Reactive oxygen species levels were determined by CellRox DeepRed (Thermo Fisher Scientific). Hundred thousand cells were incubated with culture medium containing 500nM Mitotracker DeepRed FM or 500nM CellRox DeepRed at 37℃, 5% $CO_2$ for 30-45 minutes. Cells stained by Mitotracker DeepRed were washed using PBS after staining. DeepRed fluorofore was detected using 640nm laser for excitation and 670/30nm emission filter. For the cell cycle analysis, collected cells were fixed and permeabilized using BD Cytofix/Cytoperm Fixation/Permeabilization Solution Kit (BD Biosciences) according to the manufacturer's protocol followed by staining with DAPI (Sigma-Aldrich) and PE Ki-67 (BD Biosciences).

**Quantitative real-time PCR**

Total RNA was isolated by using NucleoSpin kit (Takara Bio, Japan), and the cDNA was synthesized using ReverTra Ace (Toyobo, Japan). Quantitative real-time PCR (qPCR) was performed by using THUNDERBIRD qPCR Mix (Toyobo), with a LightCycler 480 System (Roche Applied Science, Germany). All procedures were performed according to the manufacturer's instructions. The results were normalized to the expression levels of 18s rRNA. PCR primers used for qPCR were described below (Table 2).

Table2. Primers for quantitative PCR.

| primer name | Sequence |
|---|---|
| Fbp1-Fw | ACGCTACTCCATTCTGCATG |
| Fbp1-Rv | TGACCTTGGGCATTGCAAAG |
| G6pd-Fw | AAGCCACTCCAGAAGAAAGACC |
| G6pd-Rv | GGCATTCATGTGGCTGTTGAG |
| Pgd-Fw | ATCGCTGCAAAAGTGGGAAC |
| Pgd-Rv | CAGATGAGCTGCATGTCTCC |
| Rpi-Fw | TTTTCTAAGCTGGTGCAGGTC |
| Rpi-Rv | GCTGCTCCATTCACAATTCCC |

**Generating an Evi1-overexpressing leukemia mouse model**

Bone marrow mononuclear cells of C57BL/6 mice were isolated as descried above. Sca-1 positive, c-kit positive, Lineage marker negative (KSL) cells were sorted using FACS AriaIII, precultured from one day before transduction in α-MEM (FUJIFILM Wako pure chemical corporation, Japan) supplemented with 20% FCS, 1% penicillin-streptomycin, 40ng/ml SCF, 10ng/ml IL-3, 20ng/ml IL-6, 20ng/ml TPO, and 20ng/ml Flt3-ligand and subjected to retroviral transduction with pMYs-Evi1-IRES-GFP or pMYs-mock-IRES-GFP vector. The infected cells were injected through the tail vein into sublethally irradiated (5.25 Gy) syngeneic recipient mice. After primary recipients developed leukemia, recipient mice were sacrificed and mononuclear cells of bone marrow and spleen were cryopreserved. For secondary bone marrow transplantation, approximately $5 \times 10^4$ leukemia cells were intravenously injected to sublethally irradiated (5.25Gy) syngeneic recipient mice. All animal experiments performed in this study were approved by the University of Tokyo Institutional Animal Care and Use Committee.

**Colony forming assay of p57 and Evi1 overepxressing KSL cells**

Bone marrow mononuclear cells of C57BL/6 mice were isolated as descried above. KSL cells were sorted using FACS AriaIII, precultured from one day before transduction in α-MEM (FUJIFILM Wako pure chemical corporation, Japan) supplemented with 20% FCS, 1% penicillin-streptomycin, 40ng/ml SCF, 10ng/ml IL-3, 20ng/ml IL-6, 20ng/ml TPO, and 20ng/ml Flt3-ligand and subjected to retroviral infection. After 48 hours of culture on retrovirus coated plate, cells were collected. Then GFP positive KusabiraOrange positive cells were sorted using FACS AriaIII and Sorted cells (2000 cells) in methylcellulose Methocult GF M3434 medium (Stem Cell Technologies, Canada) supplemented with 1% penicillin-streptomycin were plated in duplicate in 35mm petri dishes and incubated at 37°C, 5%CO2. The number of colonies was scored after 7 days and 2000 cells recovered from the cultured plates were replated every 7 days.

**shRNA-mediated knockdown of Fbp1, G6pd, Pgd and Rpia and colony forming assay**

Bone marrow mononuclear cells of C57BL/6 mice were isolated as descried above. KSL cells were sorted using FACS AriaIII, precultured from one day before transduction in α-MEM (FUJIFILM Wako pure chemical corporation, Japan) supplemented with 20% FCS, 1% penicillin-streptomycin, 40ng/ml SCF, 10ng/ml IL-3, 20ng/ml IL-6, 20ng/ml TPO, and 20ng/ml Flt3-ligand and subjected to retroviral infection. After 48 hours of culture on retrovirus coated plate, cells were collected. When pSIREN-RetroQ-puro vector was used these cells were further cultured in fresh medium containing 1.5 μg/ml puromycin for 24 hours. Puromycin-resistant cells were used for colony forming cell assays. When pSIREN-RetroQ-DsRed vector was used DsRed positive cells were sorted using FACS AriaIII and sorted cells were used for colony forming cell assays. Sorted cells (2000 cells) in methylcellulose Methocult GF M3434 medium (Stem Cell Technologies, Canada) supplemented with 1% penicillin-streptomycin and 1.5μg/ml puromycin if pSIREN-RetroQ-puro vector was used were plated in duplicate in 35mm petri dishes and incubated at 37°C, 5%CO2. The number of colonies was scored after 7 days and 2000 cells recovered from the cultured plates were replated every 7 days.

**shRNA-mediated knockdown of Fbp1 in Evi1 leukemia cells**

Evi1-overexpressing leukemia mice bone marrow GFP-positive cells were sorted using FACS AriaIII, precultured from one day before transduction in α-MEM supplemented with 20% FCS, 1% penicillin-streptomycin, 40ng/ml SCF, 10ng/ml IL-3, 20ng/ml IL-6, 20ng/ml TPO, and 20ng/ml Flt3-ligand and subjected to retroviral infection. Preparation of retrovirus is described separately. After 48 hours of culture on retrovirus coated plate, cells were collected and sorted using FACS AriaIII and sorted cells were used for bone marrow transplantation assays.

***In vitro* Fbp1 inhibitor administration**

Bone marrow mononuclear cells of C57BL/6 mice were isolated as descried above. KSL cells were sorted, transduced with Evi1-GFP or GFP. Then GFP-positive cells are sorted and subjected to colony-forming assay. CAY18860 (Cayman Chemical, MI) dissolved in DMSO was added to M3434 (Stem Cell Technologies). Concentration of CAY18860 and DMSO in culture medium was 0, 10 or 30μM and 0.1%, respectively.

***In vivo* Fbp1 inhibitor administration**

A fructose-1,6-bisophosphatase-1 inhibitor, CAY18860 (Cayman Chemical) dissolved in peanut oil (Sigma-Aldrich) with 5% dimethyl sulfoxide (Sigma Aldrich) was intraperitoneally administrated to Evi1 leukemia mice daily (100 µg/mouse) from 21st day to 27th day after bone marrow transplantation.

**Peripheral blood analysis**

Automated peripheral blood counts were obtained using PCE-210N (ERMA, Japan).

**RNA-sequencing analysis**

Total RNA was isolated from GFP positive, lineage negative, c-kit positive Evi1-overexpressing or the control GFP positive, lineage negative, c-kit positive bone marrow mononuclear cells by using NucleoSpin kit (Takara Bio, Japan). The quality of the RNA samples (RNA Integrity Number > 8) was validated by using Agilent 2100 Bioanalyzer (Agilent Technology, CA). For RNA library preparation, NEB Next Ultra RNA Library Prep Kit (New England Biolabs, UK) was used. RNA library samples were sequenced according to the manufacturer's protocol using an Illumina Hiseq 2000 sequencer

(Illumina, USA). Obtained sequence data were analyzed using CLC Genomics Workbench software (QIAGEN, Germany) and R (http://www.R-project.org) [49].

**Chromatin immunoprecipitation and quantitative PCR (ChIP-qPCR)**

Two-to-five million of cells were crosslinked with 1% formaldehyde at room temperature for 10 minutes, and the reaction was stopped by the addition of 80mM glycine. The fixed cells were rinsed three times with cold phosphate-buffered saline (PBS) and stored at -80°C. Cells were washed in lysis buffer (20mM Tris-HCl [pH 7.5], 10mM NaCl, 1mM EDTA, 0.2% NP-40, protease inhibitor tablets [Roche] and 1mM PMSF), resuspended in micrococcal nuclease (MNase) buffer (10mM NaCl, 10mM Thris-Hcl [pH 7.5], 2.5mM MgCl2, 0.1% NP-40, 1mM DTT, protease inhibitor tablets and 1mM PMSF) and rocked on ice for 10 minutes. After centrifugation, each pellet was resuspended in MNase buffer with 5mM CaCl2, and subjected to MNase digestion at 10000U/mL (New England Biolabs Japan, Japan). The digestion was stopped by adding EDTA after 20 minutes of incubation at 37°C and the reaction mixture was diluted with buffer-L (20mM Tris-HCl [pH 7.5], 150mM NaCl, 0.5mM EGTA, 1% Triton X-100, .0.1% sodium deoxycholate, 0.1% sodium dodecyl sulfate, protease inhibitor tablets and 1% PMSF), followed by ultrasonication with Sonifier SFX250 (Branson Ultrasonics, Japan). After sonication, 40μl of Dynabeads Protein G (Thermo Fisher Scientific) mixed with 5μg of each antibody for three hours were added to the lysates and incubated by rotating overnight, washed for five times using Magnetic stand with wash buffer (50mM HEPES-KOH [pH 7.5], 500mM LiCl, 1mM EDTA, 1% NP-40 and 0.5% sodium deoxycholate). Bound DNA fragments were eluted and quantified by subsequent qPCR. The antibodies used in ChIP assays were Monoclonal Anti-FLAG M2 antibody (F3165, Sigma-Aldrich, USA) and normal mouse IgG (Santa Cruz Biotechnology, California). Primers used in this assay are described on Table 3.

Table3. Primers for ChIP-qPCR.

| primer name | Sequence |
|---|---|
| fbp1 prm1 Fw | TTCCTTTCTGTACCCTCCACTG |
| fbp1 prm1 Rv | AAGGATCGTGTCTACCGAGTTG |
| fbp1 prm2 Fw | ACCCAATGCCCATTTCATCC |
| fbp1 prm2 Rv | ACTGTGCCAATGAGGAAGTG |
| fbp1 prm3 Fw | AAGAGTTTGGGCTGGCTGTC |
| fbp1 prm3 Rv | GAGTATGTGAACTGGAAGAGAACC |
| fbp1 prm4 Fw | TCTGTTCTGCCTAAGTTCCATG |
| fbp1 prm4 Rv | CCAGGCTTCTTCCTTTGGTTG |
| fbp1 prm5 Fw | TTCCACAAACGGGGAAGCTG |
| fbp1 prm5 Rv | CCCCACTCAGCTGTGTGAAC |
| fbp1 prm6 Fw | ATACAGGCCTCACTCTCCTAC |
| fbp1 prm6 Rv | CAAAACTTGGCCCAAAGAAGC |
| fbp1 prm7 Fw | TCCCCCAATTGAGTTCCTTTGC |
| fbp1 prm7 Rv | CACAAACCATGGACCAGTTGC |
| fbp1 prm8 Fw | TGAGAACCCCATTCAAAGGC |
| fbp1 prm8 Rv | AATCCACTCACCTCCAGTGC |
| fbp1 prm9 Fw | TGCTGGCAATTACGCAGATG |
| fbp1 prm9 Rv | TGTGTTCTGAATGCCTGCTG |
| fbp1 prm10 Fw | TGCACTTGGGAAAACAGCTG |
| fbp1 prm10 Rv | TGTTGCCCAAATGCTCAAGC |
| mGATA2 prm Fw | CAGGCTCTGGCTGGCTGCACCT |
| mGATA2 prm Rv | TTCCATACCTACGCTCTCC |
| PTEN primer3 Fw | TTTAATTTCCGAGTTTGCGTTAAT |
| PTEN primer3 Rv | AGTAAACTGCCTTGAAGCAAGTGA |

**Statistical analysis**

Statistical significance of differences between different two groups was assessed with a two-tailed unpaired Student t-test. P values <0.05 were considered significant. Overall survival of leukemia patients was depicted by Kaplan-Meier curve. Survival between two groups was compared by the log-rank test. AML patients' characteristics and RNA-seq data of The Cancer Genome Atlas (TCGA) were downloaded from cBioPortal website (http://www.cbioportal.org/) [54,55]. The overall survival of Evi1-overexpressing mice was depicted by Kaplan-Meier curve and to analyze the survival curve a log-rank test was used. Data analysis was performed using Microsoft Excel (Microsoft) and R software (http://R-project.org) [30]. Gene set enrichment analysis was performed using GSEA software [58,59].

## 【Results】

### Genome-wide transcriptome analysis induced by Evi1 overexpression in a murine leukemia model

To determine the transcriptional consequences of Evi1 overexpression and the resultant leukemic transformation *in vivo*, we compared gene expression profiles among murine bone marrow cells with or without ectopic expression of Evi1 and bone marrow leukemia cells transformed by Evi1 overexpression by RNA sequencing analysis. Bone marrow KSL cells derived from wild-type C57BL/6 mice were retrovirally transduced with Evi1-GFP or GFP and were intravenously transplanted into sublethally irradiated wild-type C57BL/6 mice (Figure 1A, B).

The fraction of long-term hematopoietic stem cells (LT-HSC, defined as CD150$^{+}$CD34$^{-}$KSL), short-term hematopoietic stem cells (ST-HSC, CD150$^{+}$CD34$^{+}$KSL), multipotent progenitor cells (MPP, CD150$^{-}$CD34$^{+}$KSL), megakaryocyte-erythroid progenitor cells (MEP, CD34$^{-}$C16/32$^{-}$Lin$^{-}$c-kit$^{+}$Sca1$^{-}$), committed myeloid progenitor cells (CMP, CD34$^{+}$C16/32$^{-}$Lin$^{-}$c-kit$^{+}$Sca1$^{-}$), and granulocyte-macrophage progenitor cells (GMP, CD34$^{-}$C16/32$^{+}$Lin$^{-}$c-kit$^{+}$Sca1$^{-}$) of GFP positive bone marrow cells isolated from transplanted mice at four weeks after transplantation were not significantly different between Evi1-GFP and GFP overexpressing groups (Figure 1C) [56]. Since lineage-negative c-kit positive cells are subdivided into these six groups of cells, we decided to compare the gene expression profiles of GFP positive, lineage-negative, c-kit positive cells of these mouse models.

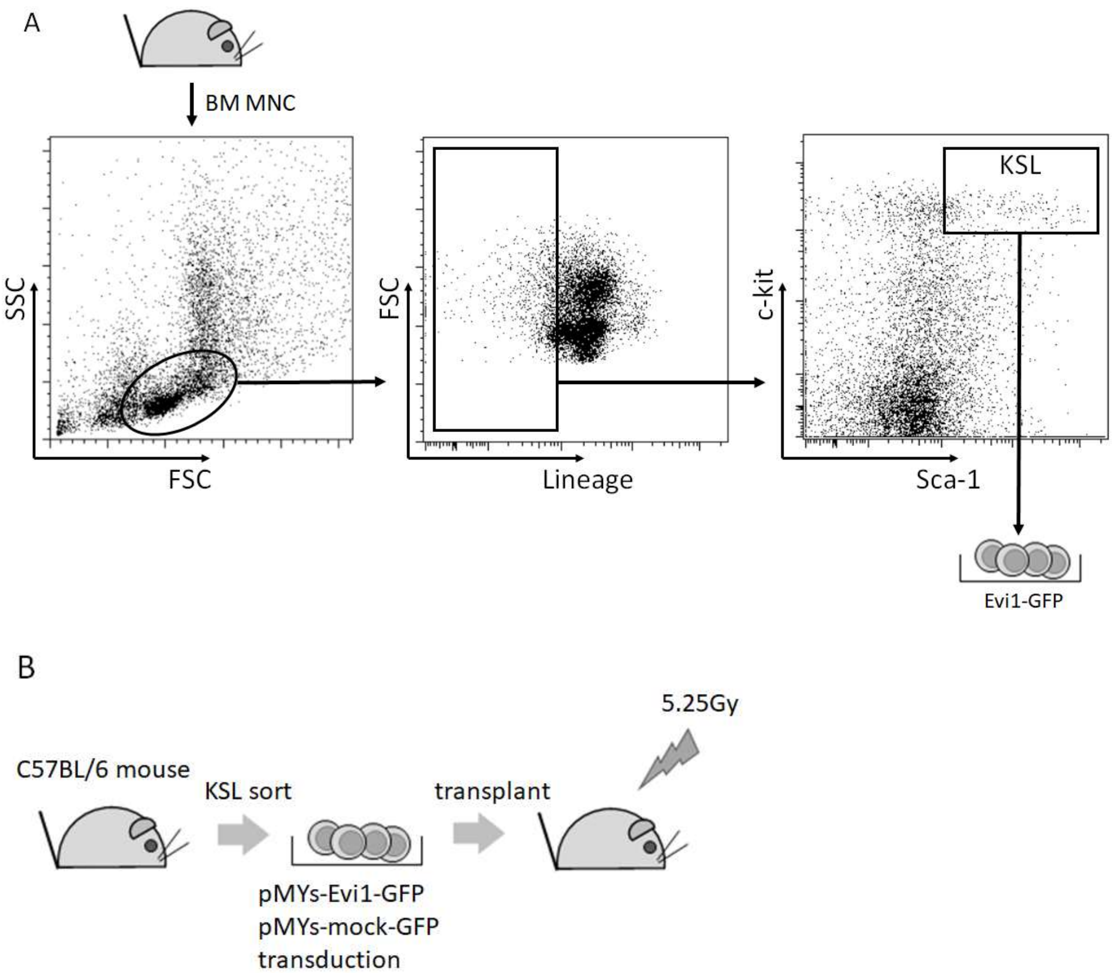

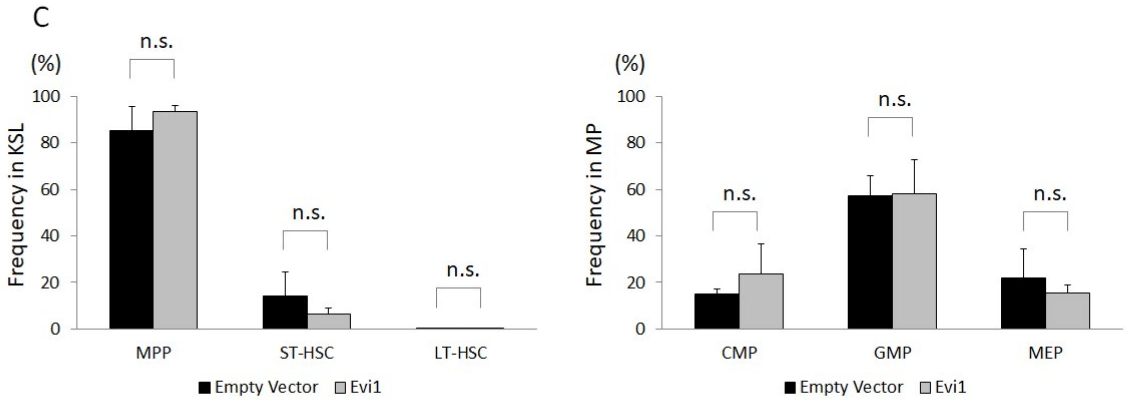


Figure 1. (A) Schematic representation of KSL sorting. (B) Schematic representation of generation of an Evi1-overexpressing leukemia mouse model. Bone marrow KSL cells collected from C57BL/6 mice were retrovirally transduced with Evi1-GFP or GFP and were intravenously transplanted into sublethally (5.25Gy) irradiated syngeneic mice. (C) Frequency of LT-HSC, ST-HSC and MPP in KSL, CMP, GMP and MEP in myeloid progenitor cells (MP, $Lin^{-}c\text{-}kit^{+}Sca1^{-}$) in GFP positive bone marrow cells collected from mice transplanted with Evi1-GFP or GFP overexpressing cells. Error bars indicate SD (n=3, unpaired *t*-test).

The GFP positive, lineage negative, c-kit positive bone marrow cells in the transplanted mice were isolated at four weeks after bone marrow transplantation (pre-leukemic stage). The transplanted mice develop overt leukemia at approximately six months after bone marrow transplantation in this model [13]. The GFP positive, lineage negative, c-kit positive bone marrow cells were also isolated from the leukemic mice, and the samples were subjected to RNA-seq analysis (Figure 2).

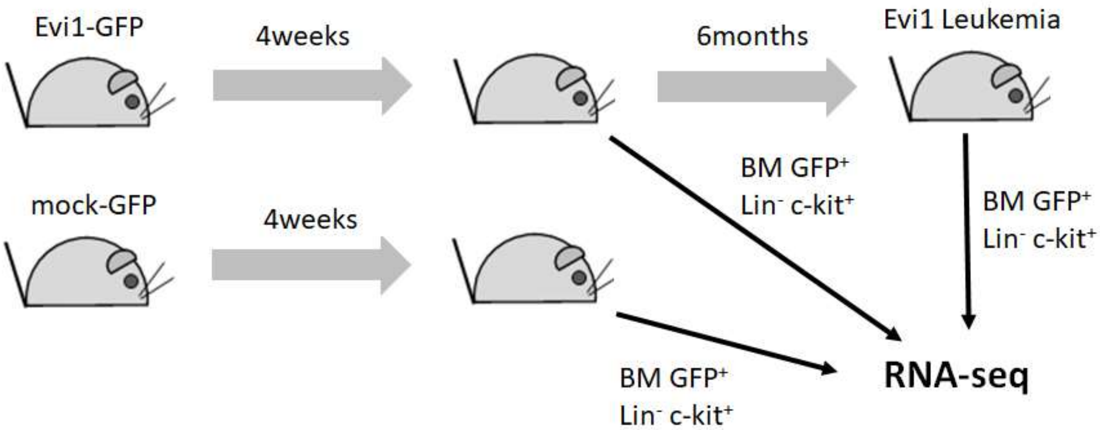


Figure 2. Schematic representation of sample preparation for RNA-seq analysis. Evi1-GFP or GFP-transduced cells were transplanted to sublethally irradiated mice. GFP-positive, lineage marker negative, c-Kit positive bone marrow cells were isolated by flow cytometry at 4 weeks (pre-leukemic phase) and 6 months (leukemic phase) after transplantation and subjected to RNA-seq analysis (n=2 in each experiment).

I compared gene expression profiles of these three groups by calculating reads per kilobase of exon model per million mapped reads (RPKM). Overall, mRNA expression levels of 1621 and 1546 genes were upregulated (RPKM ratio >2) in Evi1-overexpressing preleukemic and leukemic cells compared with the control bone marrow cells, respectively. Intriguingly, 1099 genes were upregulated (RPKM ratio >2) and 2076 genes were downregulated (RPKM ratio <0.5) in Evi1 leukemia cells isolated at 6 months after transplantation compared with Evi1-transduced cells isolated at 4 weeks after transplantation, suggesting that the Evi1-overexpressing cells acquire distinct gene expression profiles after leukemic transformation (Figure 3A, B).

Among these genes, I focused on a panel of genes with two patterns of expression changes: (i) the genes that are transiently upregulated by Evi1 overexpression and then downregulated after leukemic transformation (20 genes), and (ii) the genes that are upregulated by Evi1 overexpression and further increased in expression at a leukemia phase (11 genes) (Figure3C and Table 4 and 5). I hypothesized that these differentially expressed genes include the key factors essential for leukemogenesis induced by Evi1 overexpression.

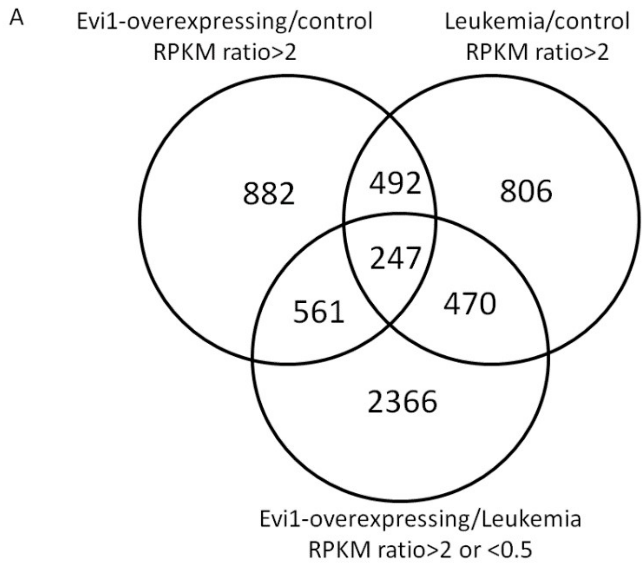

B

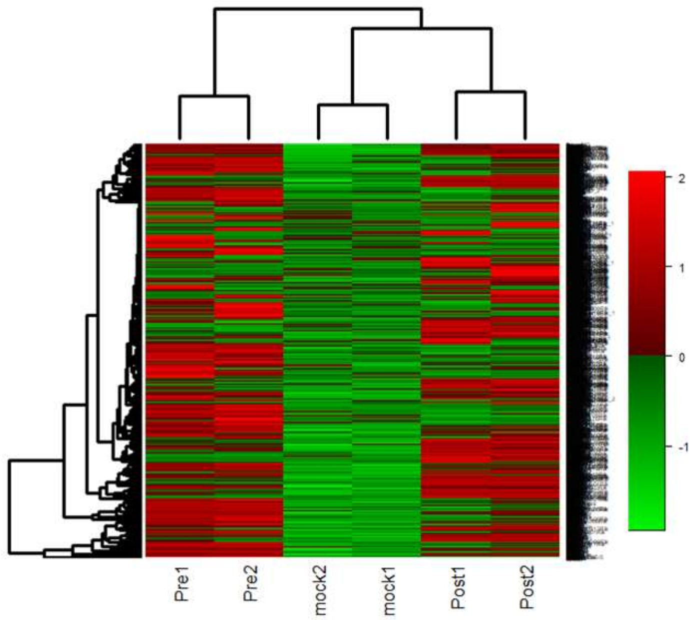


C

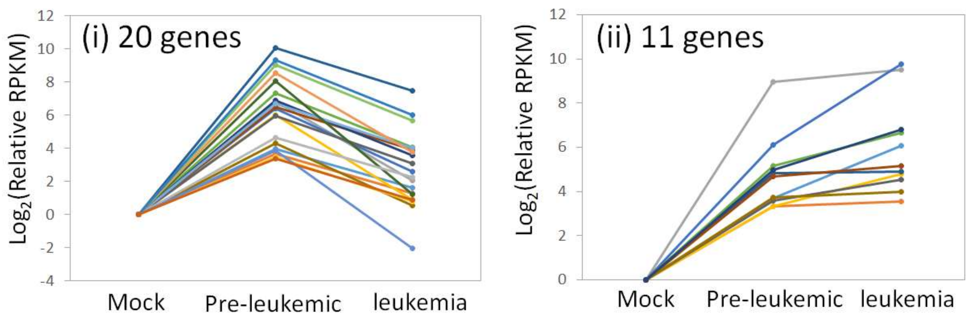


Figure 3. Evi1 leukemia cells show distinct transcriptional characteristics from Evi1-overexpresing cells. (A) Venn diagram representing an overlap of differentially expressed genes among Evi1-overexpressing pre- and postleukemic cells, and control cells. (B) Unsupervised hierarchical clustering of differentially expressed genes among the three types of the cells (more than two-fold changes in either comparison). (C) Expression changes of the genes that are downregulated (i) or upregulated (ii) after leukemic transformation in Evi1-overexpressing cells.

A.

| gene symbol | gene full name |
|---|---|
| *Wfdc21* | WAP four-disulfide core domain 21 |
| *Mcemp1* | mast cell expressed membrane protein 1 |
| *C3* | complement component 3 |
| *Camp* | cathelicidin antimicrobial peptide |
| *Cd177* | CD177 antigen |
| *Cdkn1c* | cyclin-dependent kinase inhibitor 1C |
| *Chi3l1* | chitinase 3 like 1 |
| *Fcnb* | ficolin B |
| *G0s2* | G0/G1 switch gene 2 |
| *Ifitm6* | interferon induced transmembrane protein 6 |
| *Lcn2* | lipocalin 2 |
| *Lrg1* | leucine-rich alpha-2-glycoprotein 1 |
| *Ltf* | Lactotransferrin |
| *Lyz2* | lysozyme 2 |
| *Ngp* | neutrophilic granule protein |
| *Oas2* | 2'-5' oligoadenylate synthetase 2 |
| *Prom1* | prominin 1 |
| *S100a8* | S100 calcium binding protein A8 |
| *S100a9* | S100 calcium binding protein A9 |
| *Spp1* | secreted phosphoprotein 1 |

B.

| gene symbol | Preleukemic/mock RPKM fold change | Leukemia/preleukemic RPKM fold change |
|---|---:|---:|
| *Wfdc21* | 114.5164 | 0.036852 |
| *Mcemp1* | 12.79395 | 0.187689 |
| *C3* | 15.64987 | 0.199651 |
| *Camp* | 63.71603 | 0.02955 |
| *Cd177* | 84.90232 | 0.072593 |
| *Cdkn1c* | 158.8217 | 0.106585 |
| *Chi3l1* | 1081.367 | 0.16617 |
| *Fcnb* | 91.03858 | 0.165244 |
| *G0s2* | 61.86009 | 0.137024 |
| *Ifitm6* | 20.0862 | 0.073941 |
| *Lcn2* | 118.4092 | 0.100368 |
| *Lrg1* | 105.3778 | 0.155483 |
| *Ltf* | 264.5258 | 0.008914 |
| *Lyz2* | 25.02983 | 0.189621 |
| *Ngp* | 369.9562 | 0.037279 |
| *Oas2* | 11.31442 | 0.153771 |
| *Prom1* | 14.72335 | 0.016425 |
| *S100a8* | 527.4797 | 0.09531 |
| *S100a9* | 648.5211 | 0.100917 |
| *Spp1* | 10.2475 | 0.181937 |

Table 4. (A) A list of genes transiently upregulated by Evi1 expression (fold change of RPKM >10) and then downregulated after leukemic transformation (fold change of RPKM <0.2). (B) Fold change of RPKM of each gene is shown.

A.

| Gene symbol | Gene full name |
|---|---|
| *Hbb-bt* | hemoglobin, beta adult t chain |
| *Padi4* | peptidyl arginine deiminase 4 |
| *Olfm4* | olfactomedin 4 |
| *Fbp1* | fructose-bisphosphatase 1 |
| *Npy* | neuropeptide Y |
| *Scd3* | stearoyl-coenzyme A desaturase 3 |
| *Plekhh2* | pleckstrin homology, MyTH4 and FERM domain containing H2 |
| *Retnlg* | resistin like gamma |
| *Cd200r3* | CD200 receptor 3 |
| *Krt7* | keratin 7 |
| *Upk3bl* | uroplakin 3B-like |

B.

| gene symbol | Preleukemic/mock RPKM fold change | Leukemia/Preleukemic RPKM fold change |
|---|---|---|
| *Hbb-bt* | 12.92027 | 5.182249 |
| *Padi4* | 10.06233 | 1.162111 |
| *Olfm4* | 497.3009 | 1.476184 |
| *Fbp1* | 10.01042 | 2.792997 |
| *Npy* | 68.37558 | 12.87859 |
| *Scd3* | 36.09492 | 2.816629 |
| *Plekhh2* | 28.44465 | 1.045082 |
| *Retnlg* | 25.52588 | 1.410183 |
| *Cd200r3* | 12.00863 | 1.955289 |
| *Krt7* | 13.31221 | 1.176343 |
| *Upk3bl* | 31.31763 | 3.597816 |

Table 5. (A) A list of upregulated genes by Evi1 overexpression. Genes that are upregulated by Evi-1 overexpression compared with the control bone marrow cells (more than 10-fold increase) and further increased upon leukemic transformation. (B) Fold change of RPKM of each gene is shown.

**Ectopic expression of Cdkn1c decreased serial colony forming capacity of Evi1-overexpressing mouse bone marrow cells**

The genes downregulated after leukemic transformation included the cyclin dependent kinase inhibitor 1C (*Cdkn1c*, $p57^{KIP2}$). Since $p57^{KIP2}$ inhibits cyclin complexes and negatively regulates cell proliferation, I speculated that repression of $p57^{KIP2}$ expression would contribute to leukemic transformation in an Evi1-overexpressing leukemia mouse model. To confirm that Evi1 overexpression transiently upregulates $p57^{KIP2}$, I first analyzed $p57^{KIP2}$ mRNA expression in the bone marrow c-kit$^{pos}$ Sca-1$^{pos}$ Lineage$^{neg}$ (KSL) cells transduced with Evi1-GFP or GFP (Figure 4A). Consistent with the RNA-seq results, Evi1-GFP transduced cells showed higher $p57^{KIP2}$ mRNA expression compared with GFP-transduced control cells (Figure 4B).

Since $p57^{KIP2}$ is known to counteract cell cycle progression inhibiting CDK-cyclin complexes, we analyzed the cell cycle of the bone marrow stem or progenitor cells collected from transplanted mice with Evi1-GFP or GFP overexpressing KSL cells at four weeks after transplantation [57]. Surprisingly, in Evi1-overexpressing Lin$^-$Sca1$^-$c-kit$^+$ MPs in G1 phase were significantly increased compared with GFP positive counterpart, whereas not in KSL cells (Figure 5A). In GFP$^+$Lin$^-$c-kit$^+$ cells which was subjected to RNA-seq analysis, MPs were about twice as much as KSL cells (Figure 5B). Analysis of

RNA-seq result revealed that the mRNA expression levels of other CDK interacting protein/Kinase inhibitory protein (CIP/KIP) family proteins such as p21 and p27 in Evi1-overexpressing preleukemic cells were not increased compared with control GFP-overexpressing cells (Figure 5C). These results suggest that $p57^{KIP2}$ upregulation induced by Evi1 overexpression may contribute to the cell cycle arrest in G1 phase in MPs, while its role in KSL cells are still unclear.

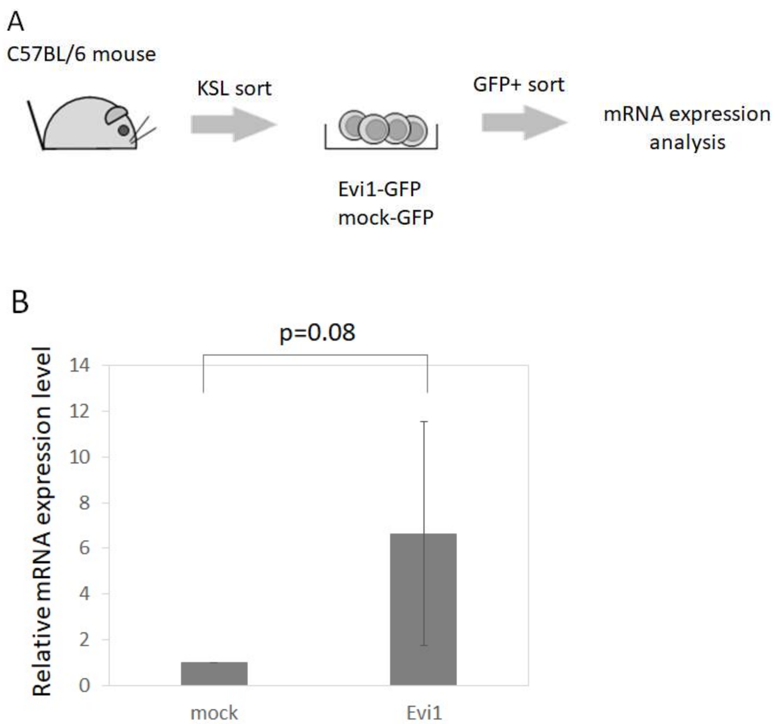


Figure 4. Cdkn1c expression is increased by Evi1 overexpression. (A) Schematic representation of mRNA expression analysis of Evi1-GFP or GFP overexpressing KSL cells. (B) Relative mRNA expression of *Cdkn1c* in KSL cells retrovirally transduced with Evi1. Error bars indicate SD (n=3, unpaired *t*-test).

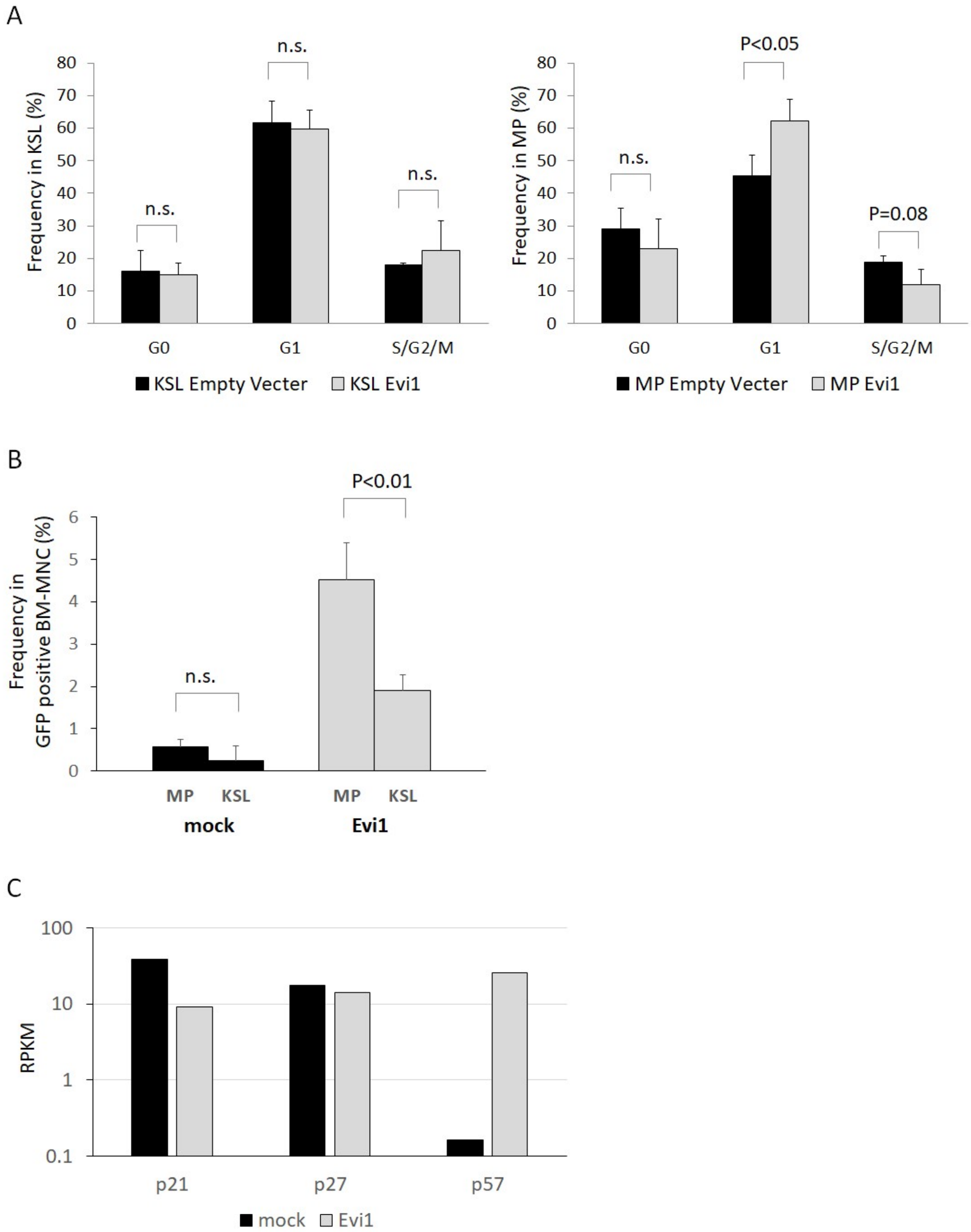


Figure 5. (A) Cell cycle analysis of GFP positive KSL or MP bone marrow cells collected from the transplanted mice with Evi1-GFP or GFP overexpressing cells at four weeks after transplantation. Error bars indicate SD (n=3 each, unpaired *t*-test). (B) Frequencies of MP and KSL cells in GFP positive bone marrow cells collected from the transplanted mice. Error bars indicate SD (n=3 each, unpaired *t*-test) (C) mRNA expression levels of p21, p27, $p57^{KIP2}$ of $GFP^{+}Lin^{-}c\text{-}kit^{+}$ cells collected from the transplanted mice are shown.

These data were retrieved from RNA-seq analysis shown in Figure 2 and Figure3 (n=2 each).

To clarify whether Cdkn1c repression contributes to Evi1 leukemogenesis, I compared colony-forming cell capacity of mouse KSL cells simultaneously transduced with Evi1-GFP and control KusabiraOrange, $p57^{KIP2}$-KusabiraOrange, or mutated $p57^{KIP2}$-KusabiraOrange. Mutated $p57^{KIP2}$ lacks a cyclin-dependent kinase (CDK) inhibitory domain, which shares significant homology with the respective CDK inhibitory domain of p21 and p27 and is necessary for the inhibition of CDK-cyclin activity.[52, 53] Evi1-overexpressing KSL cells showed higher colony-forming capacity compared with the control KSL cells (Figure 5A). When serially replated, Evi1-overexpressing KSL cells also showed higher colony-forming capacity compared with the control KSL cells (Figure 5A). Strikingly, $p57^{KIP2}$ transduced Evi1-overexpressing KSL cells showed significantly lower colony-forming capacity compared with those without $p57^{KIP2}$ transduction and the mutant $p57^{KIP2}$-transduced cells (Figure 5B and C).

A

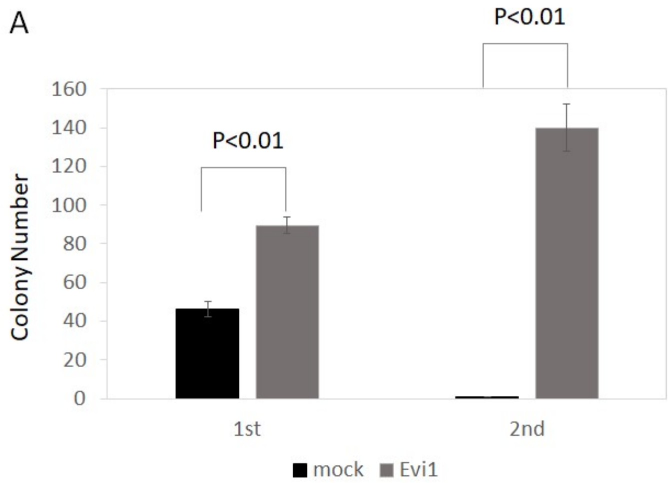
P<0.01
P<0.01
Colony Number
160
140
120
100
80
60
40
20
0
1st
2nd
mock
Evi1

B

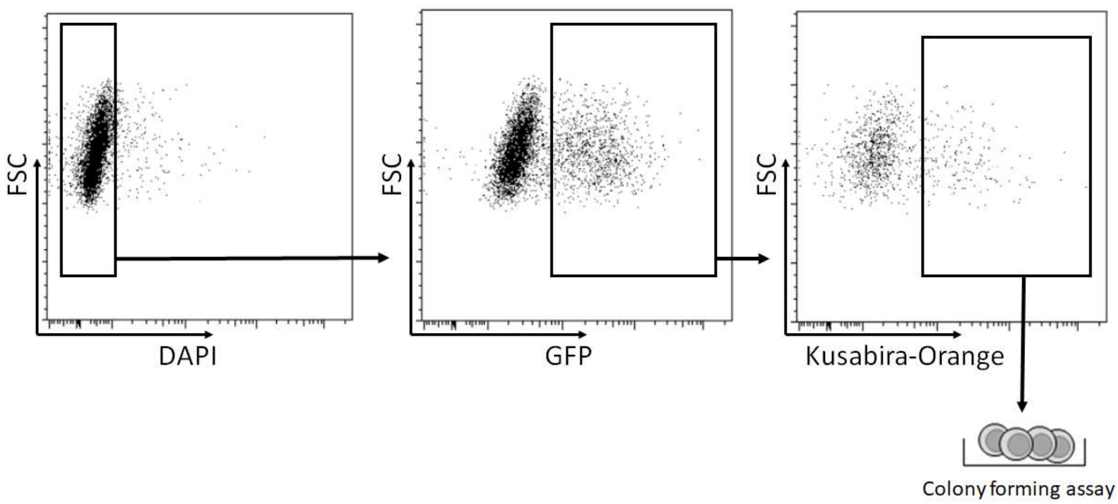
FSC
DAPI
FSC
GFP
FSC
Kusabira-Orange
Colony forming assay

C

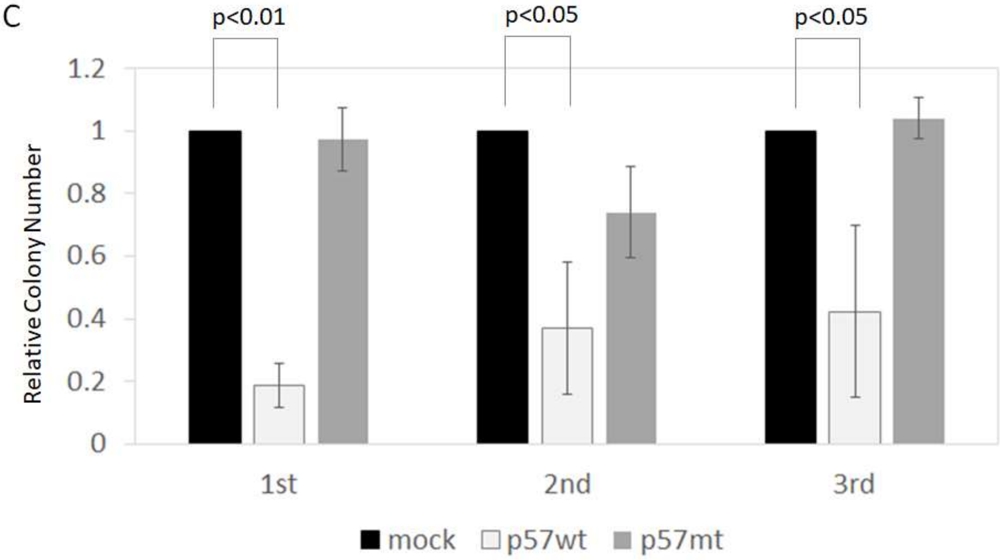
p<0.01
p<0.05
p<0.05
Relative Colony Number
1.2
1
0.8
0.6
0.4
0.2
0
1st
2nd
3rd
mock
p57wt
p57mt

Figure 5. Wild-type p57$^{KIP2}$ overexpression decreases colony-forming cell capacity of Evi1-overexpressing KSL cells. (A) Colony numbers of the Evi1-GFP or GFP-transduced KSL cells. Cells were seeded at 2000 cell per well. Error bars indicate SD (n=3 in each experiment, unpaired *t*-test). (B) Schematic representation of GFP positive and Kusabira-Orange positive cell sorting. Cells in each round were collected and sorted again for the next round colony-forming cell assay. (C) Relative colony numbers of the wild-type or mutant p57$^{KIP2}$ or mock-transduced Evi1-overexpressing KSL cells (n=4 in each experiment). Cells were seeded at 2000 cell per well. The numbers colonies relative to Evi1-GFP and mock-KusabiraOrange are shown. Error bars indicate SD (unpaired *t*-test).

When analyzed for overall survival by using the data retrieved from TCGA, I found that high Evi1 AML patients with an increased expression of $p57^{KIP2}$ showed significantly better prognosis compared with high Evi1 AML patients with low $p57^{KIP2}$ expression (Figure 6A and B). Patients' characteristics of TCGA-AML cohort patients with high Evi1 expression is shown in Table 6. Because patients with lower expression of $p57^{KIP2}$ showed poorer cytogenetic and molecular risk, and tended to undergo lower intensive chemotherapy, the prognostic impact of low $p57^{KIP2}$ may be somehow overestimated in this analysis. The same analysis focusing other genes found in Table 4 and Table 5 did not show any significant differences between high and low expression group (Figure 6A and Figure 7). *Npy, Cd200r3, Krt7, Upk3bl, Wfdc21, Fcnb, Ifitm6* and *Ngp* genes were excluded from this analysis because of the lack of appropriate human homologs or lack of RNA-seq data in TCGA-AML cohort. Taken together, although $p57^{KIP2}$ expression is transiently upregulated by ectopic expression of Evi1, its suppression may be required to accelerate leukemogenesis of Evi1-overexpressing cells.

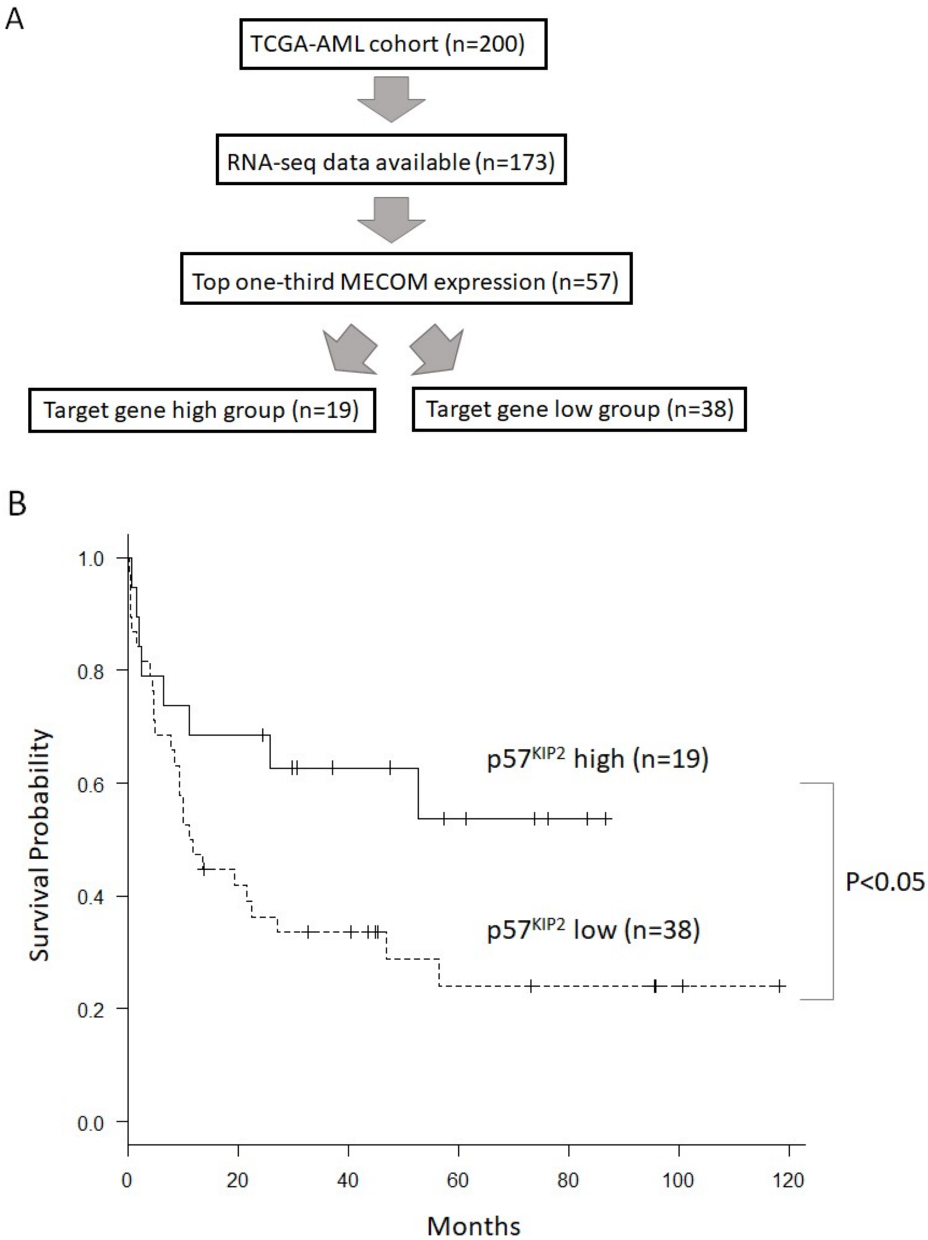


Figure 6. (A) A flow diagram of sample selection from TCGA-AML patients. (B) Analysis of overall survival in AML patients with high Evi1 expression (top one-third) (data obtained from TCGA database). Patients were grouped according to the $p57^{KIP2}$ expression levels: "$p57^{KIP2}$ high" denotes 19 patients with the top one-third CDKN1C expression levels.

| | | CDKN1C High (n=19) | CDKN1C Low (n=38) |
|---|---|---|---|
| Age | median(range) | 53(29-75) | 61(22-88) |
| Sex | male | 9(47.4%) | 21(55.3%) |
| Chemotherapy | intensive | 17(89.5%) | 24(63.2%) |
| | low intensity | 2(10.5%) | 11(28.9%) |
| | no treatment | 0(0.0%) | 3(7.9%) |
| Cytogenetic Risk | good | 9(47.4%) | 4(10.5%) |
| | intermediate | 2(10.5%) | 20(52.6%) |
| | poor | 7(36.8%) | 14(36.8%) |
| Molecular Risk | good | 8(42.1%) | 4(10.5%) |
| | intermediate | 2(10.5%) | 16(42.1%) |
| | poor | 7(36.8%) | 18(47.4%) |
| Trasnplantation | allogeneic | 6(31.6%) | 11(28.9%) |
| | autologous | 0(0.0%) | 3(7.9%) |
| | no transplantation | 13(68.4%) | 24(63.2%) |

Table 6. TCGA-AML cohort patients characteristics with high Evi1 expression (top one-third, N=57). These data were obtained from cBioPortal website. Intensive chemotherapy contained standard idarubicin plus cytarabine therapy with or without other chemotherapeutic agent. Low-intensity chemotherapy contained decitabine, lenalidomide, and low-dose cytarabine.

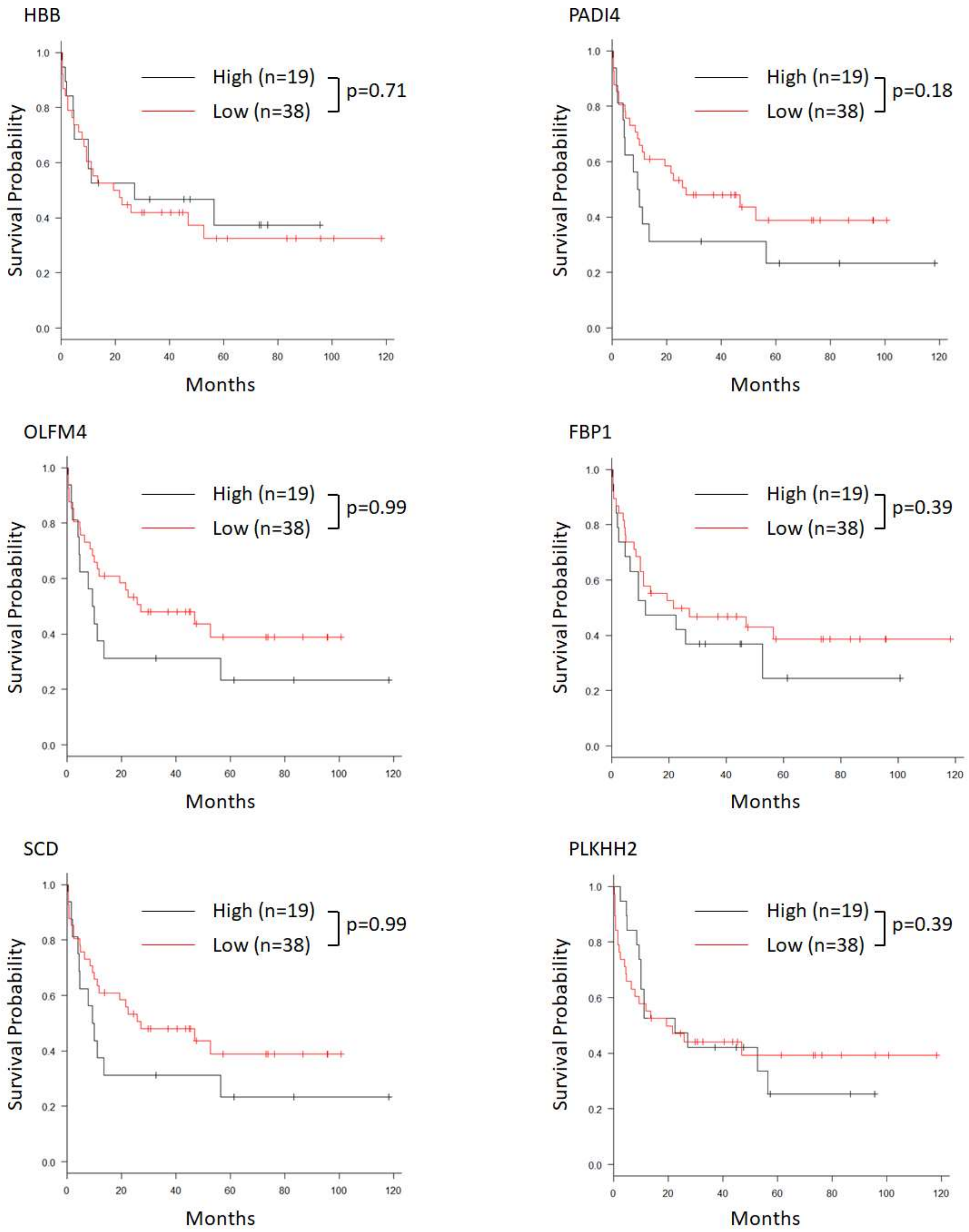
HBB
High (n=19)
Low (n=38)
p=0.71
Survival Probability
Months
PADI4
High (n=19)
Low (n=38)
p=0.18
Survival Probability
Months
OLFM4
High (n=19)
Low (n=38)
p=0.99
Survival Probability
Months
FBP1
High (n=19)
Low (n=38)
p=0.39
Survival Probability
Months
SCD
High (n=19)
Low (n=38)
p=0.99
Survival Probability
Months
PLKHH2
High (n=19)
Low (n=38)
p=0.39
Survival Probability
Months

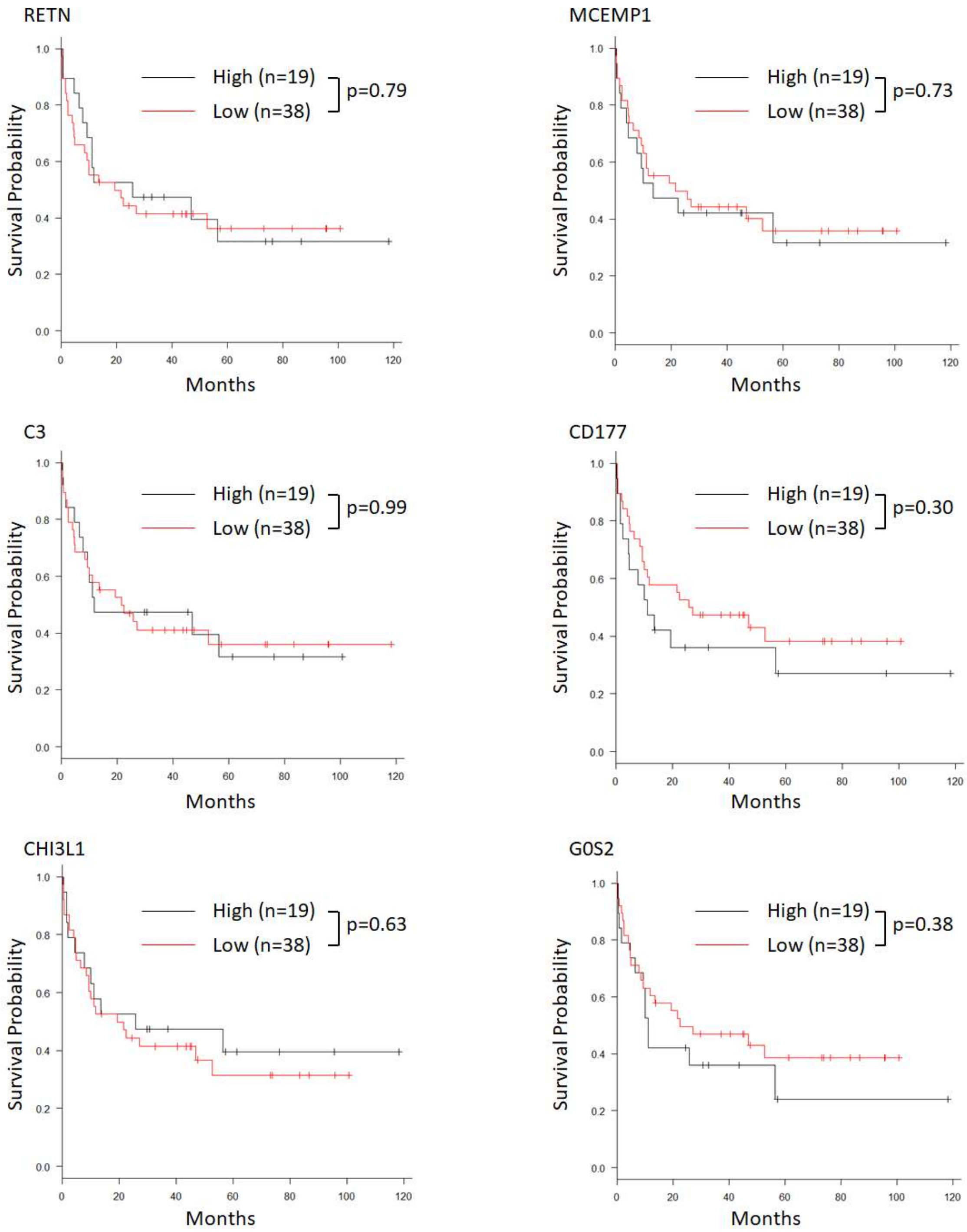
RETN
High (n=19)
Low (n=38)
p=0.79
MCEMP1
High (n=19)
Low (n=38)
p=0.73
C3
High (n=19)
Low (n=38)
p=0.99
CD177
High (n=19)
Low (n=38)
p=0.30
CHI3L1
High (n=19)
Low (n=38)
p=0.63
G0S2
High (n=19)
Low (n=38)
p=0.38
Survival Probability
Months

LCN2

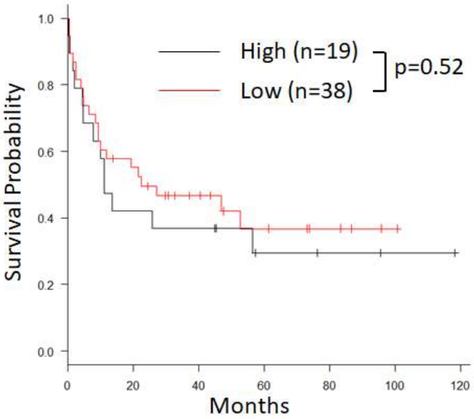


LRG1

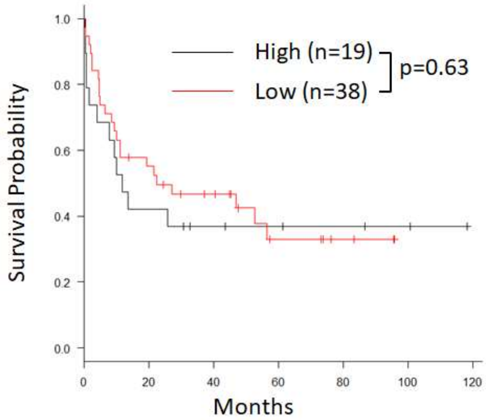


LTF

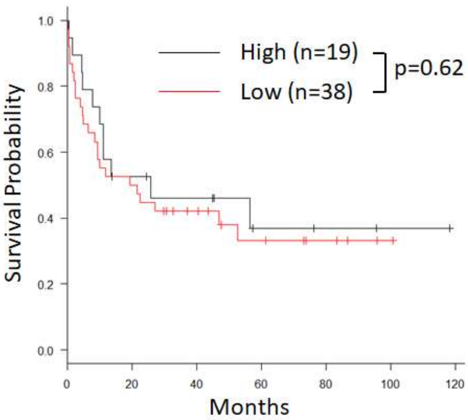


LYZ2

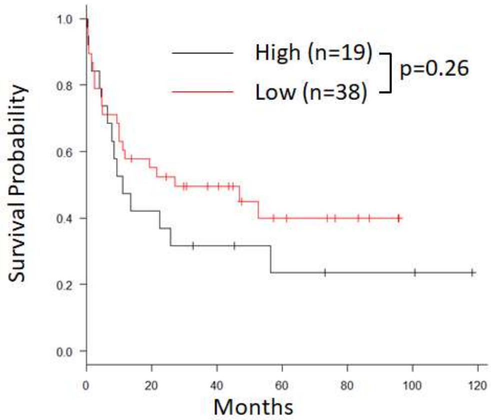


OAS2

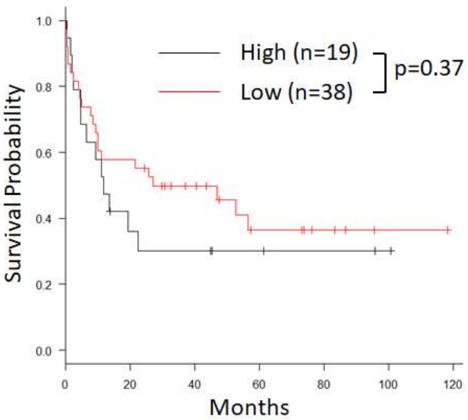


PROM1

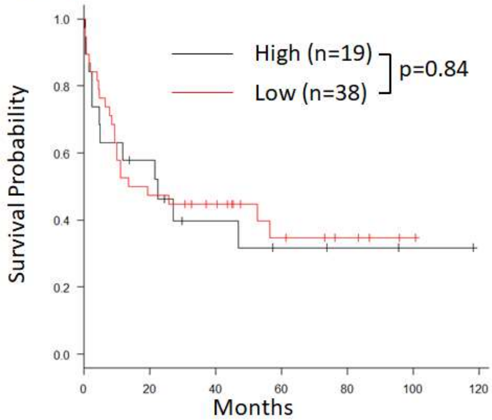

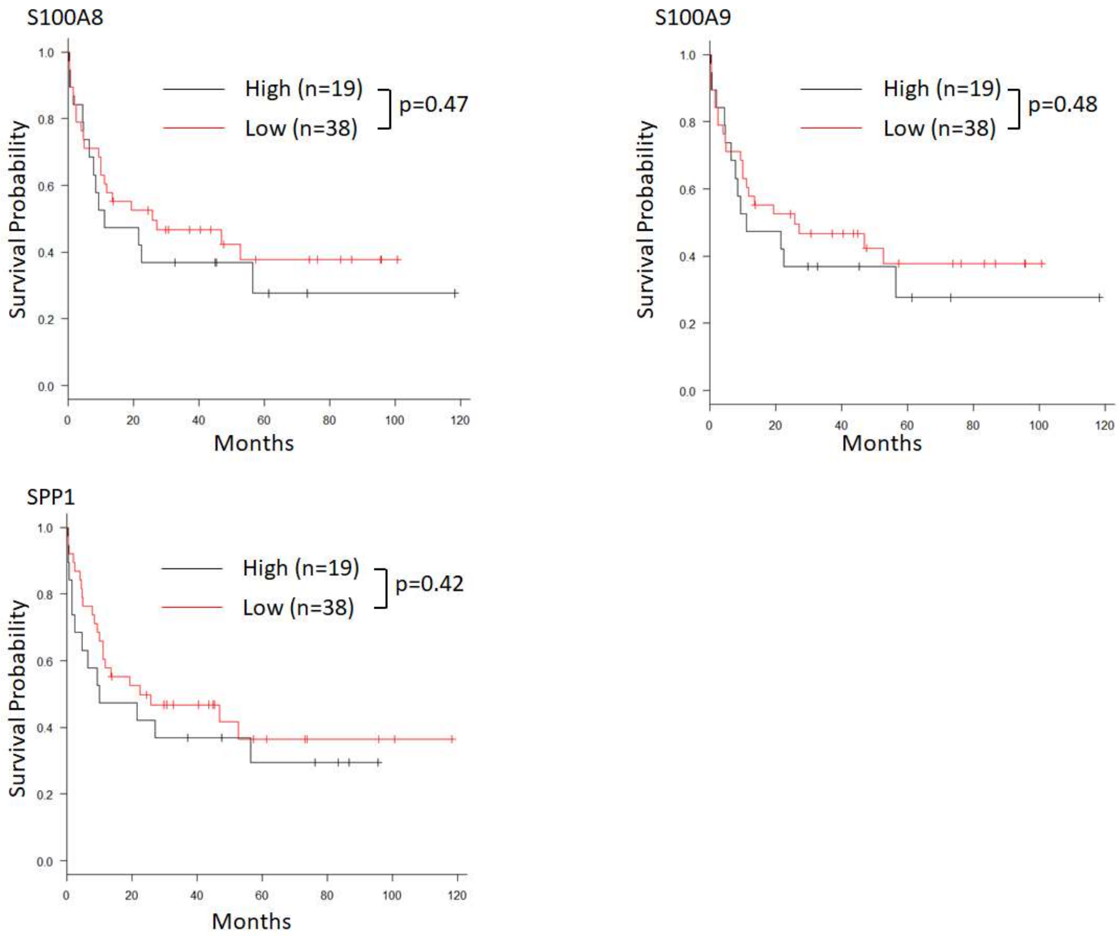


Figure 7. Analysis of overall survival in AML patients with high Evi1 expression (top one-third, n=57) (data obtained from TCGA database). Patients were grouped according to the expression levels of the concerned gene: “high” denotes 19 patients with the top one-third expression levels, “low” denotes the rest 38 patients.

**Fbp1 expression is upregulated in an Evi1-induced leukemia mouse model**

I next focused on another set of genes whose expression were further upregulated after leukemic transformation (Table 5). I found that the fructose bisphosphatase 1 (*Fbp1*) gene was included in the 11 genes extracted. FBP1 is a rate-limiting enzyme of gluconeogenesis and conversely plays a negative roles in glycolysis. In some cancers such as breast cancer, pancreatic cancer and non-small cell lung carcinoma, silencing of this enzyme is caused by various mechanisms and related to proliferation, chemoresistance and poor prognosis by increasing glycolytic flux [27, 31-35]. However, roles of Fbp1 in the context of leukemia and *in vivo* tumorigenic or tumor promoting potential of Fbp1 remains poorly understood.

Recent metabolome analysis using Evi1-overexpressing murine bone marrow cells compared with control murine bone marrow cells revealed that deoxyribonucleotide triphosphates (dNTP) are short in Evi1-overexpressing murine BM cells [24]. Since pentose phosphate pathway (PPP) is the main source of *de novo* dNTP synthesis and glucose-6-phosphate (G6P) which is converted from F6P in gluconeogenesis is the first substrate of PPP, I hypothesized that high FBP1 expression can fulfill the dNTP demand via maintenance of PPP flux (Figure 8A). Strikingly, gene set enrichment analysis of RNA-seq result of $GFP^+Lin^-c\text{-}kit^+$ bone marrow cells collected from transplanted mice with Evi1-GFP or GFP overexpressing KSL revealed that pentose phosphate pathway-related genes were enriched in the Evi1-overexpressing cells compared with control cells (Figure 8B).

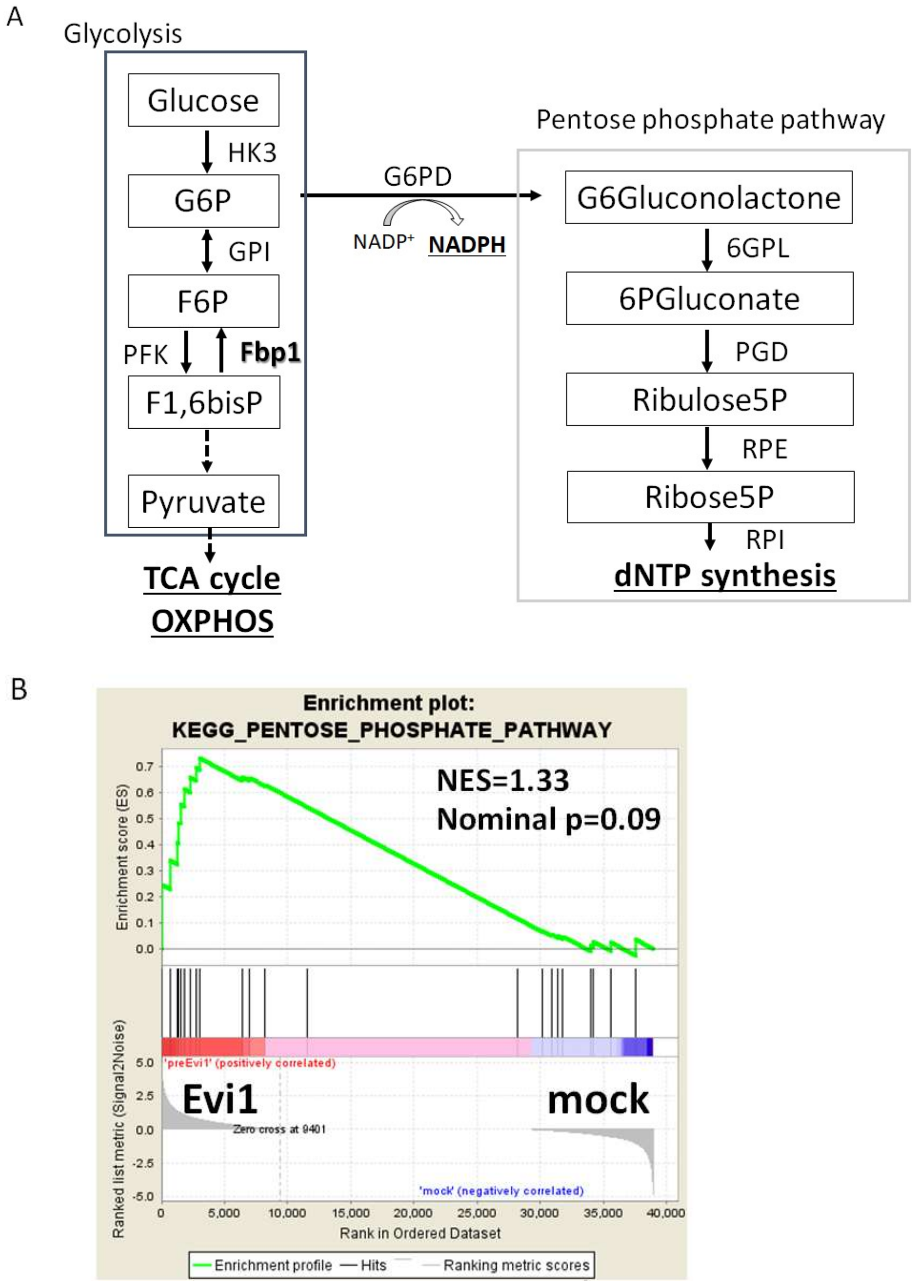


Figure 8. (A) Summary of glycolysis and pentose phosphate pathway. G6P is the branch point for proceeding to glycolysis or pentose phosphate pathway. High Fbp1 expression is assumed to increase pentose phosphate pathway flux. (B) Gene set enrichment analysis using RNA-seq data of $GFP^{+}Lin^{-}c\text{-}kit^{+}$ bone marrow cells collected from the transplanted mice with Evi1-GFP overexpressing or GFP overexpressing KSL cells at four weeks after transplantation. Geneset name: KEGG_PENTOSE_PHOSPHATE_PATHWAY was used in this analysis.

**Knockdown of PPP enzymes decreases serial colony-forming capacity of Evi1 overexpressing KSL cells**

To clarify whether PPP contributes to Evi1-overexpressing leukemia cell proliferation, I compared colony-forming cell capacity of mouse KSL cells transduced with Evi1-GFP and sh-G6pd-DsRed, sh-Pgd-DsRed, sh-Rpia-DsRed or sh-Luci-DsRed. *G6pd*, *Pgd* and *Rpia* encode the PPP enzymes G6PD, PGD and RPI, respectively. I confirmed that expression of each PPP enzyme was substantially suppressed by transduction with shRNAs (Figure 9A). Strikingly, knockdown of PGD significantly reduced colony-forming cell capacity and knockdown of each PPP enzyme significantly reduced extended colony-forming cell capacity compared with the control (Figure 9B and C). These results suggest that PPP plays a critical role in proliferation and leukemogenesis of Evi1-overexpressing leukemia.

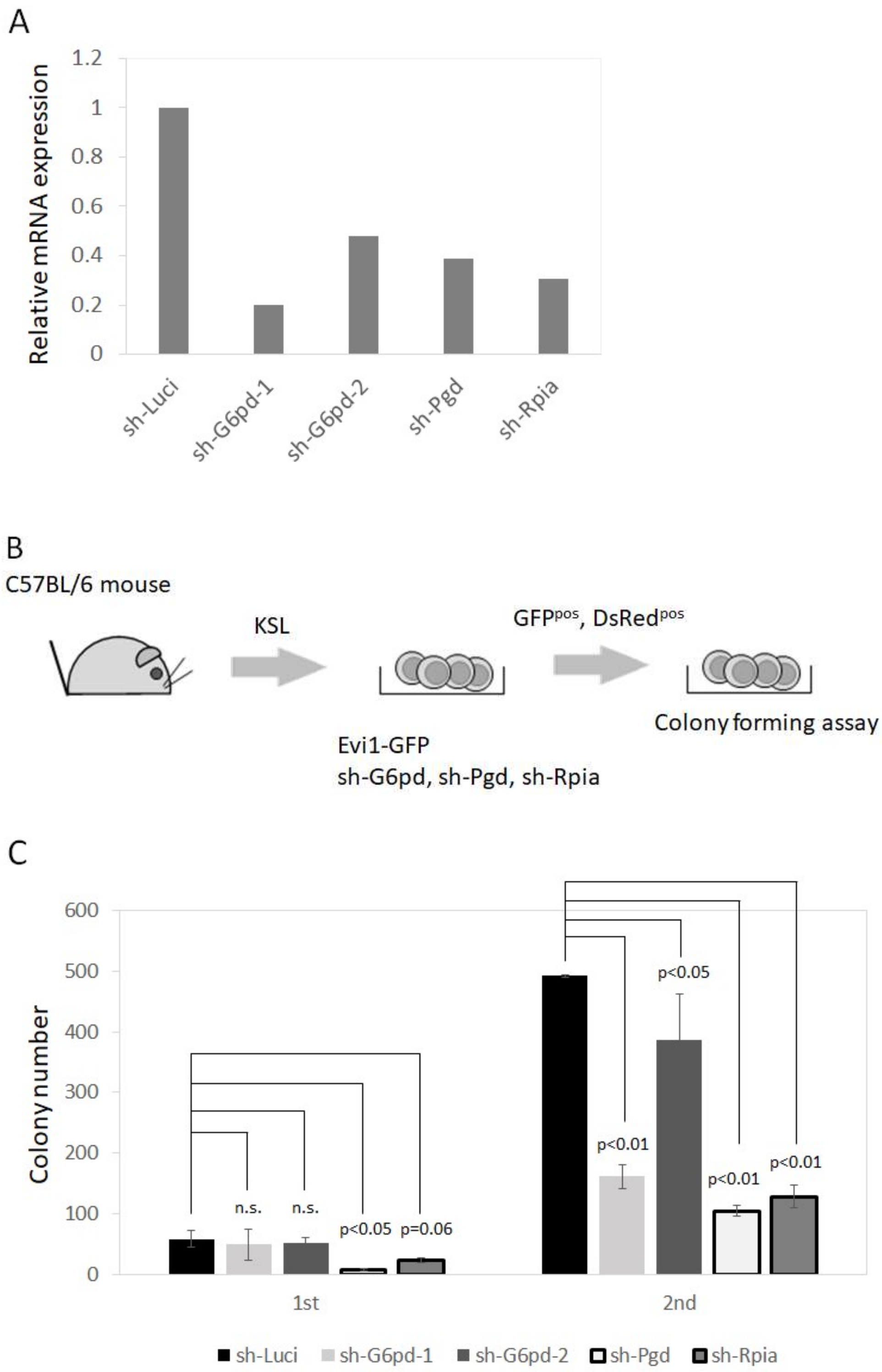
A
Relative mRNA expression
1.2
1
0.8
0.6
0.4
0.2
0
sh-Luci
sh-G6pd-1
sh-G6pd-2
sh-Pgd
sh-Rpia
B
C57BL/6 mouse
KSL
GFPpos, DsRedpos
Evi1-GFP
sh-G6pd, sh-Pgd, sh-Rpia
Colony forming assay
C
Colony number
600
500
400
300
200
100
0
n.s.
n.s.
p<0.05
p=0.06
p<0.05
p<0.01
p<0.01
p<0.01
1st
2nd
sh-Luci
sh-G6pd-1
sh-G6pd-2
sh-Pgd
sh-Rpia

Figure 9. Knockdown of PPP enzymes decreases colony-forming cell capacity of Evi1-transduced KSL cells. (A) Relative mRNA expressions of each PPP enzyme gene of Ba/F3 cell lines transduced with each shRNA vector. DsRed positive cells are sorted and subjected to qPCR. (n=2 in each experiment) (B) KSL cells isolated from the C57BL/6 mouse bone marrow cells were transduced with Evi1-GFP and sh-G6pd, sh-Pgd, sh-Rpia or sh-luciferase (control). GFP positive and DsRed positive cells were then sorted and analyzed for colony-forming cell capacity. For the second assay, cells are collected from 35mm dishes and GFP positive and DsRed positive cells were sorted again. (C) Colony numbers of KSL cells transduced with Evi1-GFP and each shRNA vectors compared with the control shRNA-transduced cells were shown.. Error bars indicate SD (n=4 in each experiment, unpaired *t*-test).

**Fbp1 expression is directly regulated by Evi1**

I analyzed Fbp1 mRNA expression in Evi1-transduced mouse KSL cells in comparison with control KSL cells by qPCR. Consistent with the RNA-sequencing results, Fbp1 mRNA levels were significantly increased in Evi1-transduced cells (Figure 10A). To interrogate whether Evi1 directly regulates the Fbp1 expression, I next assessed enrichment of EVI1 in the promoter and enhancer region of Fbp1 by performing ChIP-qPCR analysis. A total of 10 primers were designed in the well-conserved sites between the human and mouse genome within the promoter and enhancer region of Fbp1 (-5kb-30kb from the transcription start site) (Figure 10B. Evolutionary conserved sites across species were explored using rVista 2.0 [36]. In ChIP-qPCR, 32D mouse myeloblast-like cells transduced with FLAG-Evi1 IRES-GFP or GFP were used and primers targeting GATA2 promoter and PTEN promoter were used as positive controls [13, 37]. As shown in Figure 10C, Evi1 tended to be enriched in primers #5, #9 and #10 targeting the Fbp1 upstream region. Taken together, these data suggest that Evi1 directly binds to the Fbp1 promoter and enhancer, and upregulate expression of Fbp1.

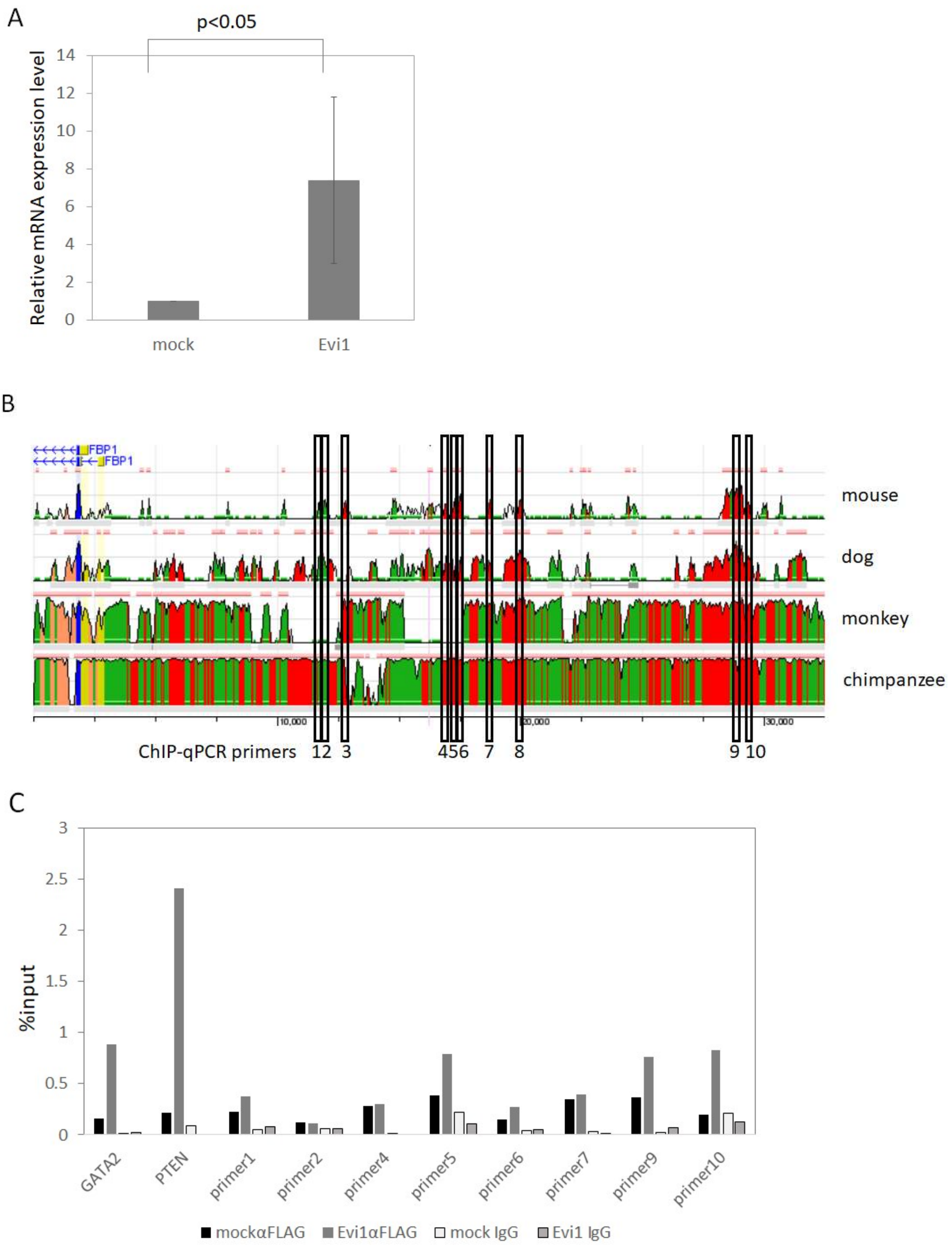


Figure 10. (A) Relative mRNA expression of *Fbp1* in KSL cells retrovirally transduced with Evi1. Error bars indicate SD (n=3, unpaired *t*-test) (B) Schematic representation of mouse Fbp1 promoter and enhance region, possible Evi1 binding site predicted by rVista 2.0 and ten primers for ChIP assays. (C) ChIP-qPCR analysis for Flag-Evi1-GFP or GFP-expressing 32D cells by using an anti-FLAG antibody (αFLAG or normal IgG) (n=1 each). Primers targeting the GATA2 and PTEN promoter regions were used as positive controls.

**Knockdown of Fbp1 decreases intracellular ROS levels in Evi1-overexpressing leukemia cells *in vivo***

Since Fbp1 is a predominant enzyme of gluconeogenesis, increased expression of Fbp1 may suppress a glycolytic flux, which is one of main sources of adenosine 5'-triphosphate (ATP) in cancer cells [38,39]. I hypothesized that elevation of Fbp1 alternatively upregulate oxidative phosphorylation (OXPHOS) to generate ATP. Since higher OXPHOS flux leads to increased ROS generation, I analyzed intracellular ROS levels of Evi1-overexpressing leukemia cells *in vivo*. To examine ROS levels of Evi1-overexpressing leukemia cells with or without Fbp1 knockdown, I generated secondarily transplanted Evi1-overexpressing leukemia mouse model. In this model, GFP positive fraction of Evi1-overexpressing leukemia cells collected from the bone marrow were sorted, subjected to transduction of shFbp1-DsRed or shLuci-DsRed expressing retrovirus, then again GFP positive DsRed positive cells were sorted and transplanted into sublethally irradiated normal C57BL/6 mice (Figure 11A). After leukemic transformation of secondarily transplanted Evi1-overexpressing leukemia mice, DsRed-positive peripheral blood mononuclear cells were sorted and subjected to CellRox DeepRed or Mitotracker DeepRed staining. Interestingly, sh-Fbp1-transduced Evi1 leukemia cells showed lower ROS levels compared with the control Evi1 leukemia cells (Figure 11B and C). These data suggest that Fbp1 upregulation by Evi1 overexpression results in a high OXPHOS flux state in leukemia cells *in vivo*.

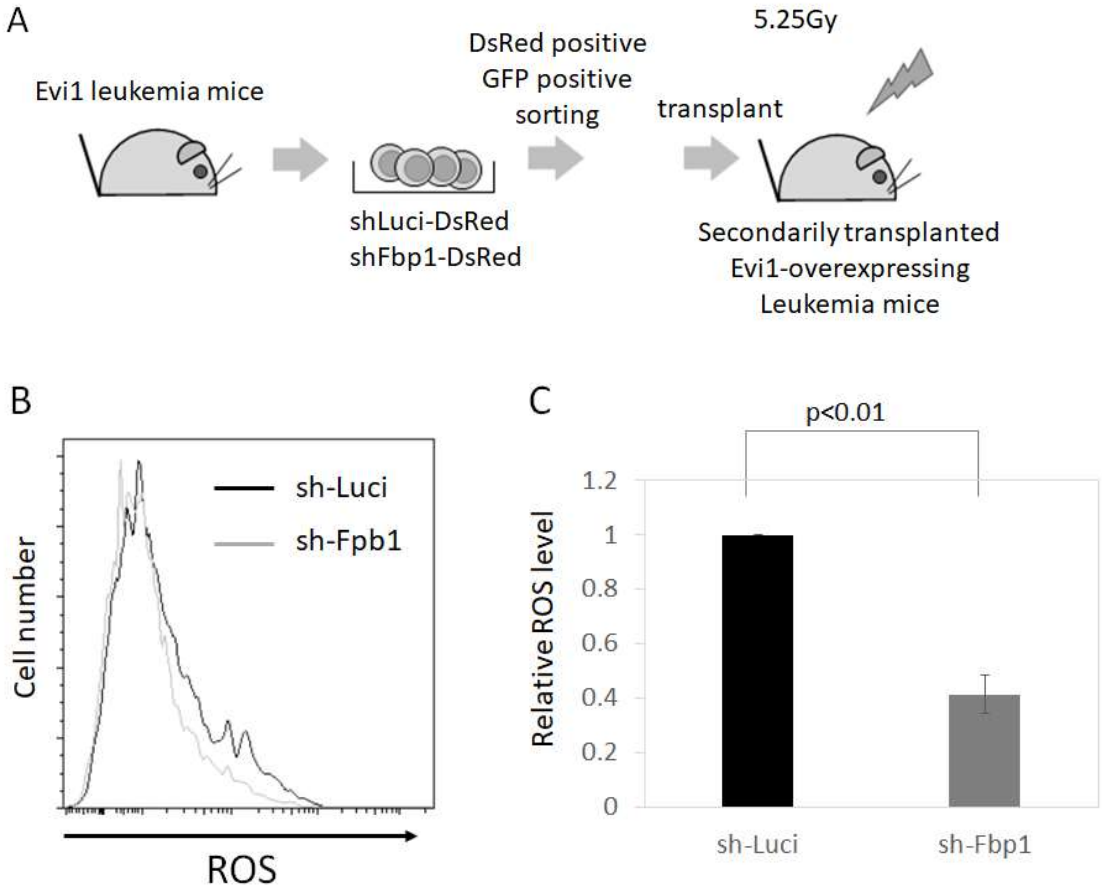


Figure 11. Fbp1 knockdown in Evi1-overexpressing leukemia cells decrease intracellular ROS levels. (A) Bone marrow GFP-positive cells were isolated from the Evi1-overexpressing leukemia cells, transduced with sh-Fbp1-DsRed or sh-Luci-DsRed (control). DsRed positive GFP positive cells were sorted and transplanted into sublethally irradiated normal C57BL/6 mice. (B) Representative flow cytometry analysis of intracellular ROS in Evi1 overexpressing leukemia cells transduced with sh-Fbp1 or sh-luciferase (control). ROS was detected by CellRox DeepRed staining. (C) Relative ROS levels measured by CellRox DeepRed in Evi1 overexpressing leukemia cells transduced with sh-Fbp1 or sh-luciferase. Error bars indicate SD (n=3 in each group, unpaired *t*-test).

**Knockdown of Fbp1 decreases colony-forming cell capacity of Evi1-overexpressing cells and Evi1 leukemia cell expansion *in vivo***

I further tested whether Fbp1 contributes to Evi1-overexpressing leukemia cell proliferation or leukemogenesis. I confirmed that Fbp1 expression was successfully suppressed by transduction with shRNA (Figure 12A). Knockdown of Fbp1 significantly reduced serial colony-forming cell capacity in mouse KSL cells transduced with Evi1-GFP (Figure 12B and C). Compared to knockdown of PPP enzymes, the effect of knockdown of Fbp1 on colony-forming cell capacity seemed to be less. These results are compatible to our hypothesis that knockdown of Fbp1 indirectly decreases PPP activity via the control of G6P metabolism.

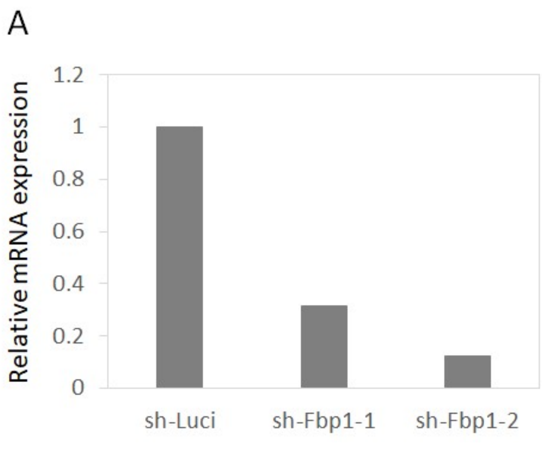

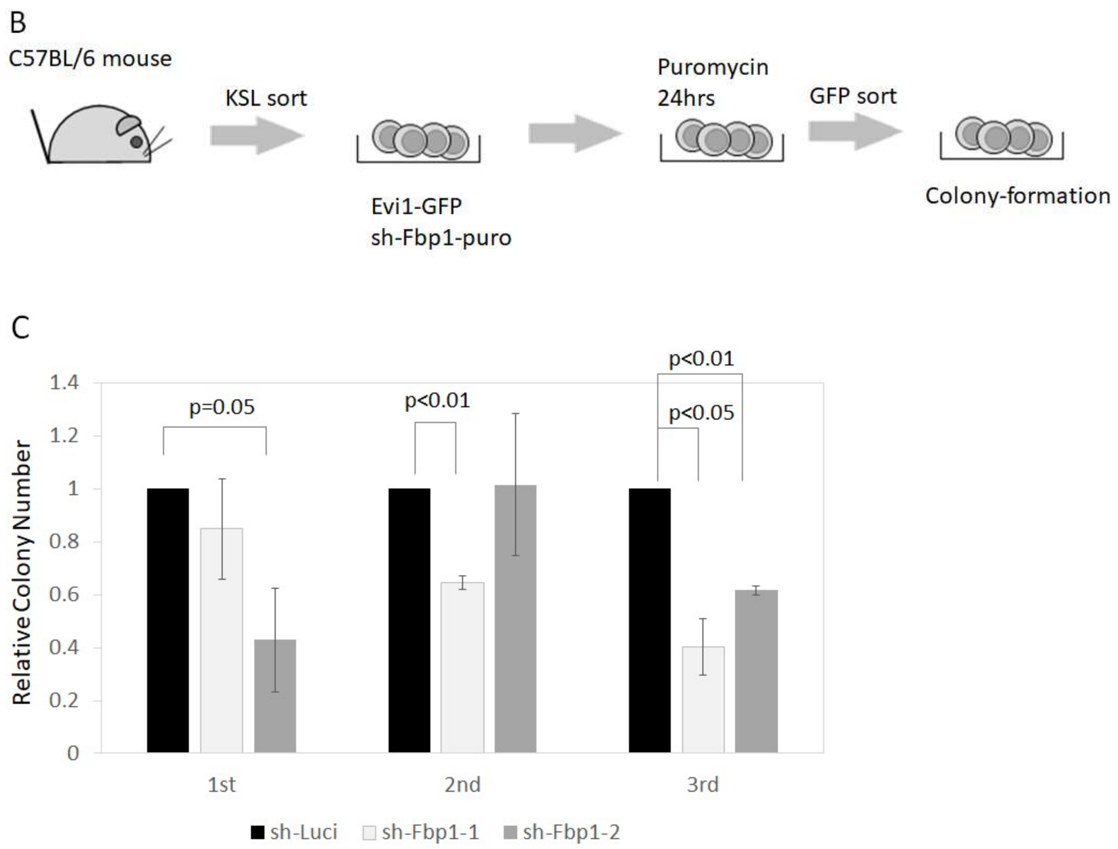


Figure 12. Knockdown of Fbp1 decreases colony-forming cell capacity of Evi1-transduced KSL cells. (A) Relative mRNA expression of Fbp1 of Ba/F3 cell lines transduced with Fbp1 knockdown vector is shown. Ba/F3 was transduced with shFbp1. After 24 hours of puromycin selection, GFP positive cells are sorted and subjected to qPCR. (n=2 each) (B) KSL cells isolated from the C57BL/6 mouse bone marrow cells were transduced with Evi1-GFP and sh-Fbp1 or sh-luciferase (control), and the shRNA-transduced cells were selected by puromycin for 24 hours. The GFP positive cells were then sorted and analyzed for colony forming-cell capacity. (C) Relative colony numbers of KSL cells transduced with Evi1-GFP and sh-Fbp1compared with the control shRNA-transduced cells were shown (n=3 in each experiment, unpaired *t*-test). Error bars indicate SD.

Next, I analyzed the effect of Fbp1 knockdown on Evi1-overexpressing leukemia cells *in vivo* (Figure 13A). Strikingly, shRNA-mediated knockdown of Fbp1 in Evi1 overexpressing leukemia cells significantly delayed the onset of Evi1 leukemia (Figure 11A). As shown in figure 12B, flow cytometric analysis of peripheral blood of mice secondarily transplanted with Evi1-overexpressing cells revealed that increased white blood cells are not necessarily GFP positive nor DsRed positive although transplanted cells were GFP positive and DsRed positive. To evaluate the effect of Fbp1 knockdown on Evi1-overexpressing leukemia cells, I compared DsRed positive cell frequencies of peripheral blood mononuclear cells of mice transplanted with shFbp1 transduced Evi1-overexpressing leukemia cells to shLuci transduced counterpart. Consistent with the result of white blood cell count, shRNA-mediated knockdown of Fbp1 in overexpressing leukemia cells significantly decreased frequencies of DsRed positive cell (Figure 13C).

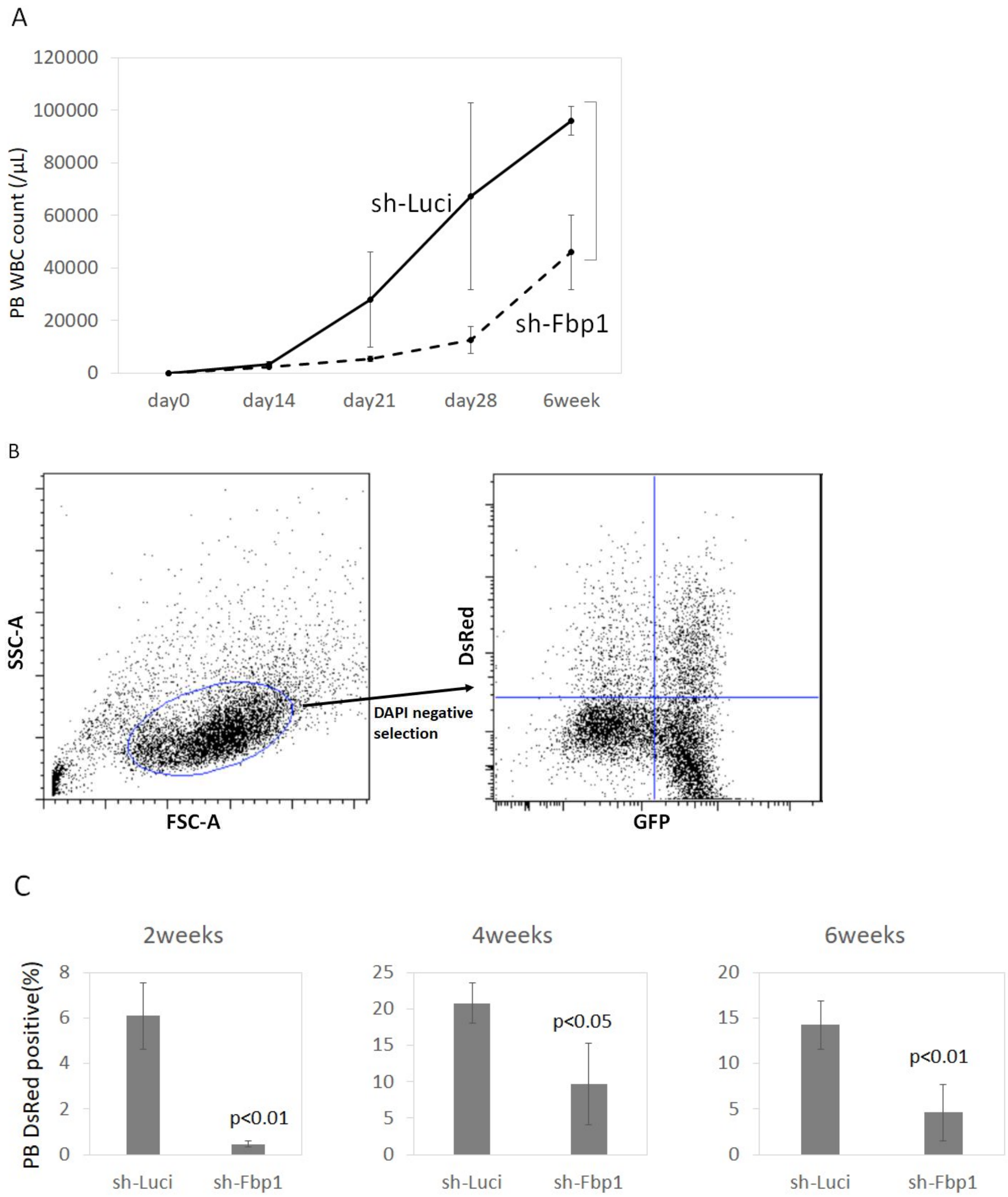


Figure 13. Knockdown of Fbp1 delays Evi1 leukemia progression. (A) Peripheral blood white blood cell counts of the transplanted mice at the indicated time points are shown. (n=4 in each group, unpaired *t*-test) Error bars indicate SD. (B) Representative flow cytometric plot of peripheral blood chimerism analysis. (C) Frequency of DsRed-positive cells within the peripheral blood mononuclear cells is shown (n=4 in each group, unpaired *t*-test). Error bars indicate SD.

Finally, I tested whether pharmacologic inhibition of FBP1 can suppress Evi1-overexpressing leukemia cell proliferation. The effect of an FBP1 inhibitor CAY18860 on colony-forming cell capacity of Evi1-overexpressing KSL cells or control KSL cells was analyzed [60, 61]. Interestingly, CAY18860 decreased serial colony-forming cell capacity of Evi1-overexpressing KSL cells whereas not those of control KSL cells (Figure 14A). To evaluate the effect of CAY18860 *in vivo*, CAY18860 was administered to the mice that were secondarily transplanted with Evi1-overexpressing leukemia cells (Figure 14B). Flow cytometry analysis revealed that FBP1 inhibition significantly reduced leukemia burden, consistent with the data obtained by the knockdown of Fbp1 (Figure 14C). Although these results clearly indicate the anti-Evi1-overexpressing leukemia effect of Fbp1 inhibitor, the overall survival of the mice that were secondarily transplanted with Evi1-overexpressing leukemia cells was not significantly prolonged by administration of Fbp1 inhibitor (Figure 14D). This negative result can be explained by two reasons. First, the pharmacokinetics of CAY18660 *in vivo* is not well understood. Although one of derivatives of CAY18660, compound 4.4 (depicted in [61]) has thirty times lower EC50 in inhibiting FBP1 than CAY18660 and is shown to have sufficient ability to inhibit FBP1 *in vivo*, this compound was difficult to obtain. More effective compounds can have a higher anti-leukemic effect *in vitro* and *in vivo*. Second, since the sample size of this experiment was small, it was possible that the difference couldn't be detected. Taken together, these results suggest that Fbp1 upregulation contributes to progression of Evi1-overexpressing leukemia cells. Inhibition of Fbp1 or its downstream molecules in the pentose phosphate pathway would be a promising therapeutic target against Evi1 high leukemia.

A

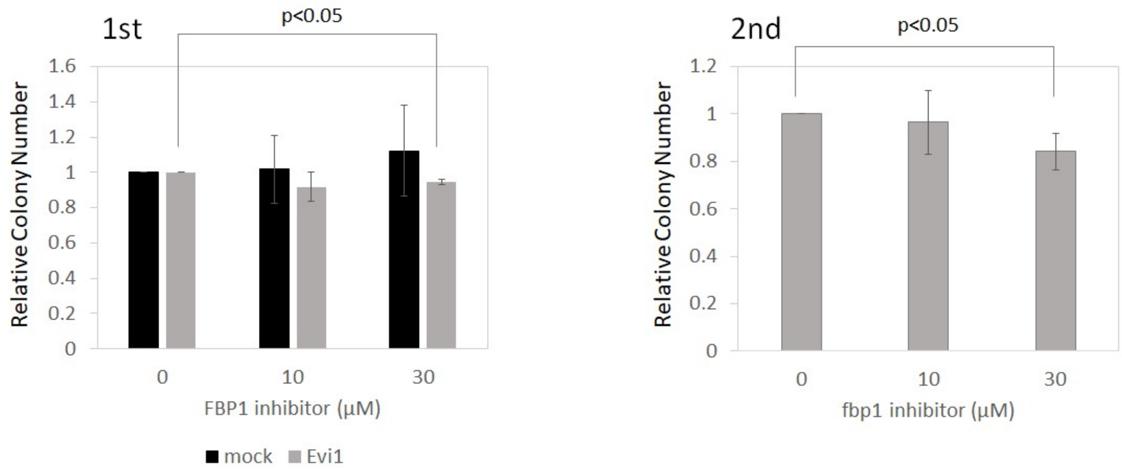

1st
p<0.05
1.6
1.4
1.2
1
0.8
0.6
0.4
0.2
0
Relative Colony Number
0
10
30
FBP1 inhibitor (μM)
mock
Evi1
2nd
p<0.05
1.2
1
0.8
0.6
0.4
0.2
0
Relative Colony Number
0
10
30
fbp1 inhibitor (μM)


B

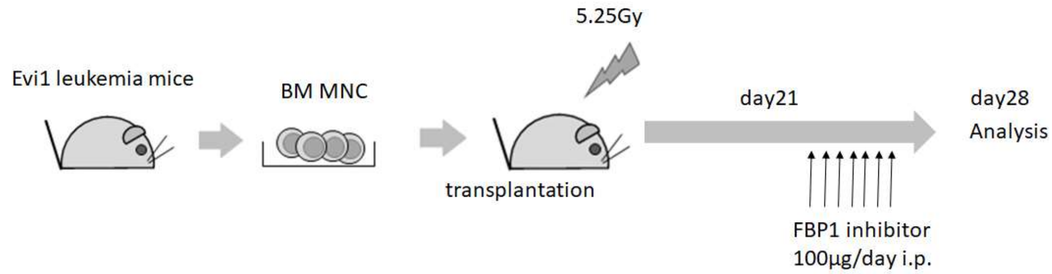

5.25Gy
Evi1 leukemia mice
BM MNC
day21
day28
Analysis
transplantation
FBP1 inhibitor
100μg/day i.p.


C

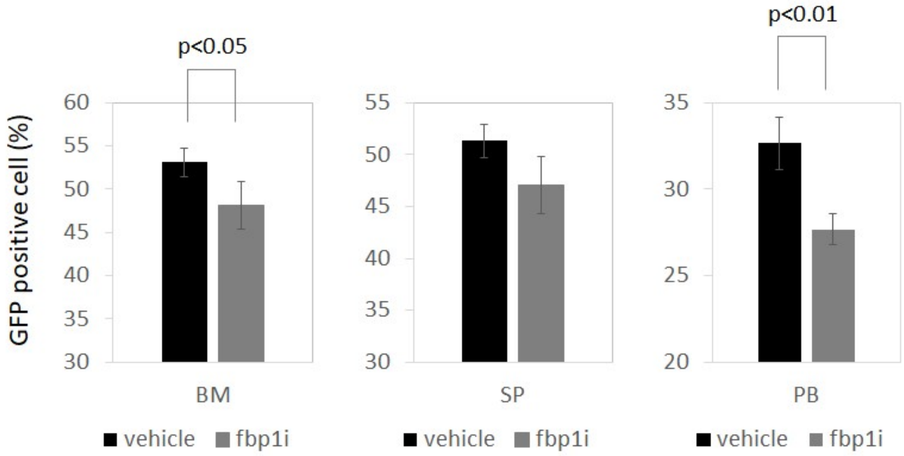

p<0.05
p<0.01
GFP positive cell (%)
60
55
50
45
40
35
30
BM
vehicle
fbp1i
55
50
45
40
35
30
SP
vehicle
fbp1i
35
30
25
20
PB
vehicle
fbp1i

D

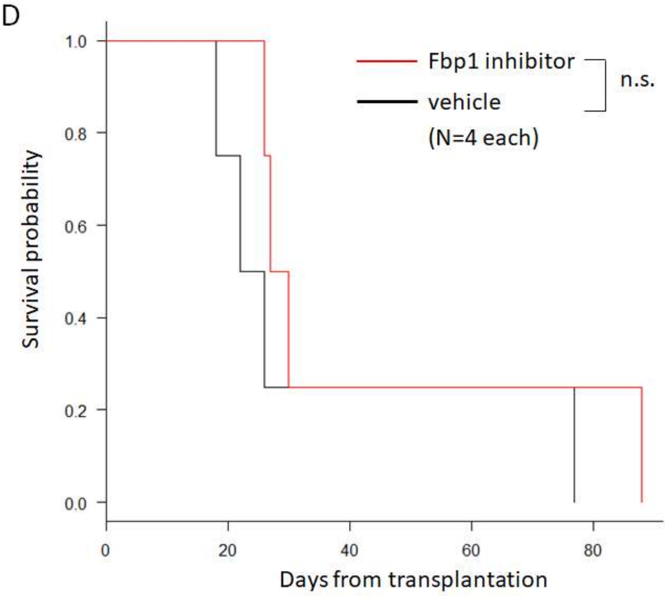


Figure 14. An FBP1 inhibitor decreases colony-forming cell capacity of Evi1-overexpressing KSL cells and decreases leukemia burden in Evi1 leukemia mice. (A) KSL cells isolated from the bone marrow of C57BL/6 mice were transduced with Evi1-GFP or GFP. GFP-positive cells were then sorted and analyzed for colony-forming cell capacity. Relative colony numbers of Evi1-overexpressing KSL cells and control KSL cells are shown on the left panel (n=3 in each experiment, unpaired *t*-test). Relative colony numbers of replated Evi1-overexpressing KSL cells are shown on the right panel (n=3 in each experiment, unpaired *t*-test). Colony numbers were adjusted to the data of the cells treated with vehicle (FBP1 inhibitor 0μM). Cells were seeded at 2000 cells per well. Error bars indicate SD. (B) Leukemia cells isolated from the bone marrow of Evi1 leukemia mice were intravenously transplanted into sublethally irradiated normal C57BL/6 mice (day 0). An FBP1 inhibitor CAY18860 was intraperitoneally injected daily into the leukemic mice on day 21-27. (C) On day 28, the mice were sacrificed and analyzed for the frequency of GFP-positive cells in the bone marrow (BM), spleen (SP) and peripheral blood (PB) (n=4 in each experiment, unpaired *t*-test). Error bars indicate SD. (D) Kaplan-Meier curves representing the survival of vehicle or Fbp1 inhibitor treated mice that were secondarily transplanted with Evi1-overexpressing leukemia cells. (n=4 in each group, log-rank test).

## 【Discussion】

In this study, I addressed molecular profiles of Evi1-overexpressing AML cells. I found that Evi1 overexpression and subsequent leukemic transformation result in genome-wide gene expression changes in mouse bone marrow stem/progenitor cells *in vivo.* Although it is well known that Evi1 causes various transcriptomic alterations by directly binding to DNA and recruitment of other transcription factors and chromatin-modifying enzymes, comparative analysis of gene expression profiles in Evi1-overexpressing pre-leukemia and leukemia cells at different time points has not been performed [13-19, 51]. Among the genes upregulated by ectopic expression of Evi1, I identified two patterns of expression changes; the genes that were suppressed in expression after leukemic transformation, and those that were further upregulated after leukemic transformation. Investigation of these genes seems to be promising because the genes in the former group may contribute to suppression of leukemic transformation and the genes in the latter group may include the transcriptomic target genes of Evi1.

Among the genes downregulated at the leukemia phase, I found that repression of $p57^{KIP2}$ may contribute to Evi1-mediated leukemogensis. $p57^{KIP2}$ belongs to the CIP/KIP family of cyclin-dependent kinase inhibitors and causes cell cycle arrest mostly in G1 phase and a proapoptotic effect in cancer cell lines, and is considered a tumor suppressor gene [40-45]. In line with this idea, reduction of $p57^{KIP2}$ contributes to tumorigenesis in hepatocellular carcinoma, lung cancers and adrenal tumors. In these cancers, inactivation of $p57^{KIP2}$ by somatic deletion or genetic mutations, promoter DNA methylation, repressive histone modification such as Histone 3 lysine 27 tri-methylation, miRNA mediated regulation and proteasomal degradation was reported. $p57^{KIP2}$ also plays a critical role to maintain stemness of hematopoietic stem cells by PR-domain of Mecom mediated transcriptional activation [48]. High expression of $p57^{KIP2}$ in myelodysplastic syndrome (MDS) and secondary AML is reported to be associated with poor prognosis [46, 47]. However, a role of $p57^{KIP2}$ in leukemogenesis and leukemia progression is still largely unknown. Evi1 has controversial effects on proliferative capacity of leukemia cells. While some studies showed that Evi1 promotes leukemia cell proliferation, others report that Evi1 overexpression contributes to quiescence in leukemia cell lines. Dynamic changes of $p57^{KIP2}$ expression levels upon Evi1 overexpression may underlie these paradoxical effects. Downregulation of $p57^{KIP2}$ at later time points may be induced by Evi1-dependent and independent changes of epigenetic profiles such as histone modifications or DNA methylation and other transcription factors. Further studies are required to clarify molecular mechanisms of $p57^{KIP2}$ downregulation in Evi1-overexpressing leukemia cells.

Among the genes with further upregulation upon leukemia transformation, I focused on Fbp1 and showed that Fbp1 is a direct transcriptional target of Evi1 and contributes to Evi1-overexpressing AML progression. My results suggest that high Fbp1 expression alters glucose metabolism in Evi1-overexpressing leukemia cells, drives glucose metabolism from glycolysis to PPP and OXPHOS. Fbp1 has been reported as a tumor suppressor gene in other solid cancers [27, 31-35]. In this context, high Fbp1 expression decreases glycolysis flux indispensable for quick ATP supply in low-oxygen environment to which many highly proliferative cancers are exposed. Suppression of Fbp1 is related to cell proliferation, chemoresistance and metastasis. Contrary to these previous reports, I demonstrated that suppression of Fbp1 decreases colony-forming cell capacity *in vitro* and leukemia progression *in vivo*. It would be possible that maintenance of PPP has a pivotal role for survival or proliferation of Evi1-overexpressing leukemia cells. Consistent with this hypothesis, I showed that knockdown of PPP enzymes significantly decreased colony forming-cell capacity of Evi1-overexpressing KSL cells. There have also been controversial reports in a role of Fbp1 in the PPP activity. In hepatocellular carcinoma and breast cancer cell lines, Fbp1 expression decreases PPP flux by slowing whole glucose metabolism *in vitro*, whereas Fbp1 overexpression does not necessarily compromise glucose intake [32, 33]. Further studies are needed to test whether PPP flux is upregulated through increased Fbp1 expression mediated by Evi1 overexpression. In addition to PPP, increased Fbp1 expression may result in activation of OXPHOS to compensate for decreased anaerobic glycolysis for ATP generation. My results that knockdown of Fbp1 decreases intracellular ROS levels in Evi1-overexpressing leukemia cells is consistent with this hypothesis. Previous reports also showed that breast cancer cell lines overexpressing Fbp1 possess elevated OXPHOS flux, and pancreatic carcinoma cell lines downregulate OXPHOS activity upon Fbp1 suppression *in vitro* [32, 35]. Although consistent with my hypothesis, these experiments were performed *in vitro*. It may provide better insights by analyzing the OXPHOS activity *in vivo*. Interestingly, elevated OXPHOS seemed to be related to chemotherapy resistance [50]. Fbp1 upregulation in Evi1-overexpressing leukemia cells may contribute to their chemo-resistant properties. The relationship between Fbp1 and $p57^{KIP2}$ has not been reported before. In this leukemia mouse model, energy and nucleotide demand due to cell cycle progression mediated by $p57^{KIP2}$ suppression may be fulfilled by metabolic alteration caused by Fbp1 upregulation, since Fbp1 upregulation would activate PPP, the most important pathway of *de novo* nucleotide synthesis, and OXPHOS.

In summary, the present study shows that (i) $p57^{KIP2}$ downregulation may contribute to leukemic transformation in Evi-1 overexpressing cells, and (ii) high Fbp1 expression contributes to Evi1 leukemia progression through altering glucose metabolism profiles. These results provide multiple promising therapeutic targets for Evi1$^{high}$ leukemia refractory to chemotherapy (Figure 14).

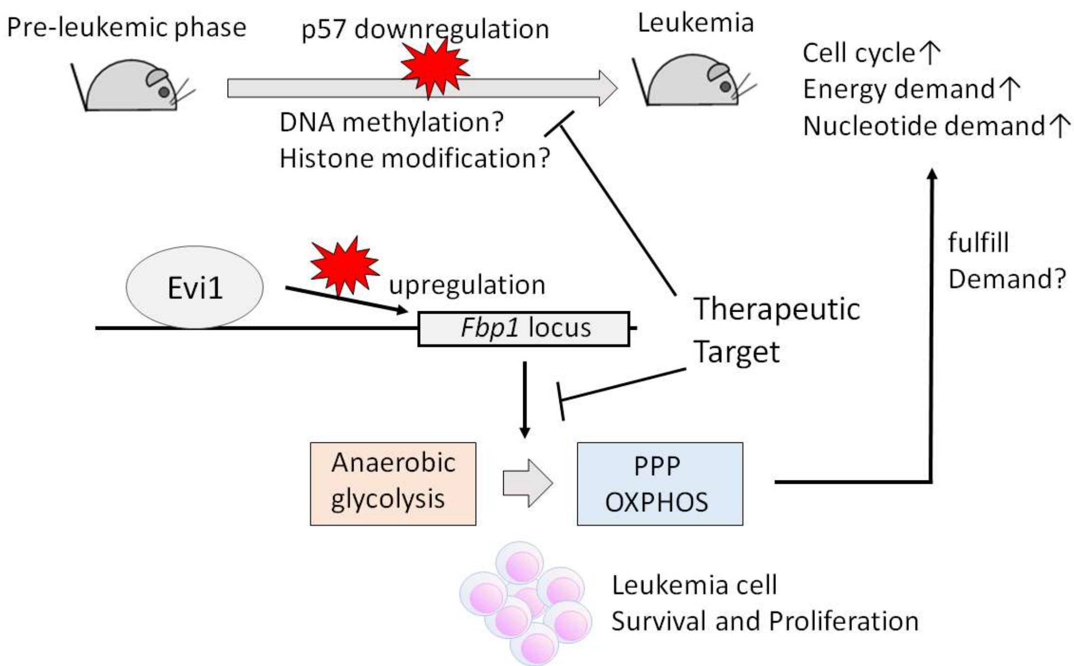


Figure 14. A proposed model showing the roles of p57 and Fbp1 in Evi1-overexpressing leukemia. While p57 downregulation promotes leukemic transformation, progressive upregulation of Fbp1 mediated by Evi1 alters glucose metabolism and contributes to leukemia. Hypothetical explanations are written with question marks.

【Acknowledgements】

I would like to express my deepest appreciation to Professor Mineo Kurokawa for supervising the entire study and providing me the opportunity to write this paper. I would also like to thank Dr. Yuki Kagoya for giving me critical advices in performing experiments and writing this paper. I also thank Dr. Junji Koya for performing RNA-seq analysis, cell-cycle analysis and analysis of stem/progenitor cell frequencies of mouse bone marrow cells, kindly providing these data and advising me throughout this research. I also express my gratitude to Dr. Yosuke Masamoto, Dr. Masashi Miyauchi, Dr. Kensuke Takaoka, Dr. Yoshiki Sumitomo, Dr. Megumi Yasunaga, Dr. Takashi Higo and Dr. Akira Honda for giving many advices and stimulating my research. I also thank Fumie Ueki, Keiko Tanaka, Satomi Muroi and Yoko Hokama for their technical support. I also thank Dr. Shunya Arai, Dr. Fumihiko Nakamura, Dr. Kumi Nakazaki, Dr. Kazuhiro Toyama and Dr. Masahiro Uni for their continued support. I also thank Y. Goto for providing $p57^{KIP2}$ and mutated $p57^{KIP2}$ complementary DNA, T. Nakamura for pMYs-mouse Evi1-IRES-GFP and T. Kitamura for Plat-E packaging cells.

【References】

1. H Döhner, DJ Weisdorf, and CD Bloomfield. Acute Myeloid Leukemia. 373, 1136-1152 (2015).

2. S Barjesteh van Waalwijk van Doom-Khosrovani, C Erpelinck, WL van Putten, . High EVI1 expression predicts poor survival in acute myeloid leukemia: a study of 319 de novo AML patients. Blood. 101, 837-845 (2003).

3. PJ Valk, RG Verhaak, MA Beijen, CA Erperlinck, S Barjesteh van Waalwijk van Doom-Khosrovani, JM Boer, HB Beverloo, MJ Moorhouse, PJ van der Spek, B Löwenberg, R Delwel. Prognostically useful gene-expression profiles in acute myeloid leukemia. N Engl J Med. 350, 1617-1628 (2004).

4. S Lugthart, E van Drunen, Y van Norden, A van Hoven, CA Erpelinck, PJ Valk, HB Beverloo, B Löwenberg, R Delwel. High EVI1 levels predict adverse outcome in acute myeloid leukemia: prevalence of EVI1 overexpression and chromosome 3q26 abnormalities underestimated. Blood. 111, 4329-4337 (2008).

5. S Groschel, S Lugthart, RF Schlenk, PJ Valk, K Eiwen, C Goudswaard, WJ van Putten, S Kayser, LF Verdonck, M Lübbert, GJ Ossenkoppele, U Germing, I Schmidt-Wolf, B Schlegelberger, J Krauter, A Ganser, H Döhner, B Löwenberg, K Döhner, R Delwel. High EVI1 expression predicts outcome in younger adult patients with acute

myeloid leukemia and is associated with distinct cytogenetic abnormalities. J Clin Oncol. 28, 2101-2107 (2010).

6. E Papaemmanuil, M Gerstung, L Bullinger, VI Gaidzik, P Paschka, ND Roberts, NE Potter, M Heuser, F Thol, N Bolli, G Gundem, PV Loo, I Martincorena, P Ganly, L Mudie, S McLaren, S O'Meara, K Raine, DR Jones, JW Teague, AP Butler, MF Greaves, A Ganser, K Döhner, RF Schlenk, H Döhner, and PJ Campbell. Genomi Classification and Prognosis in Acute Myeloid Leukemia. N Engl J Med. 375, 2023-2036 (2016).
7. YZ Qin, T Zhao, HH Zhu, J Wang, JS Jia, JS Jia, YY Laai, XS Zhao, HX Shi, YR Liu, H Jiang, XJ Huang, and Q Jiang. High EVI1 Expression Predicts Poor Outcomes in Adult Acute Myeloid Leukemia Patients with Intermediate Cytogenetic Risk Receiving Chemotherapy. Med Sci Monit. 24, 758-767 (2018).
8. D Grimwade, RK Hills, AV Moorman, H Walker, S Chatters, AH Goldstone, K Wheatley, CJ Harrison, and AK Burnett. Refinement of cytogenetic classification in acute myeloid leukemia: determination of prognostic significace of rare recurring chromosomal abnormalities among 5876 younger adult patients treated in the United Kingdom Medical Research Council trials. Blood 116, 354-365 (2010).

9. Z Hu, S Hu, C Ji, Z Tang, B Thakral, S Loghavi, LJ Medeiros, W Wang. 3q26/EVI1 rearrangement in myelodysplastic/myeloproliferative neoplasms: An early event associated with a poor prognosis. Leuk Res 65, 25-28 (2018).
10. SH Swerdlow, E Campo, NL Harris, ES Jaffe, SA Pileri, H Stein, J Thiele, DA Arber, RP Hassejian, MM Le Beau, A Orazi, and R Siebert. WHO Classification of Tumours of Haematopoietic and Lymphoid Tissues, Revised 4th Edition. 138-139 (2018).
11. S Katayaa, M Suzuki, A Yamaoka, N Keleku-Lukwete, F Katsuoka, A Otsuki, S Kure, JD Engel, and M Yamamoto. Blood. 130, 908-919 (2017).
12. H Yamazaki, M Suzuki, A Otsuki, R Shmizu, EH Bresnick, JD Engel and M Yamamoto. A Remote GATA2 Hematopoietic Enhancer Drives Leukemogenesis in inv(3)(q21;q26) by Activating EVI1 Expression. Cancer Cell. 25, 415-427 (2014).
13. A Yoshimi, S Goyama, N Watanabe-Okochi, Y Yoshiki, Y Nannya, E Nitta, S Arai, T Sato, M Shimabe, M Nakagawa, Y Imai, T Kitamura, and M Kurokawa. Evi1 represses PTEN expression and activities PI3K/AKT/mTOR via interactions with polycomb proteins. Blood. 31, 3617-3628 (2011).
14. E Ayoub, MP Wilson, KE Mcgrath, AJ Li, BJ Frisch, J Palis, LM Calvi, Y Zhang, and AS Perkins. EVI1 overexpression reprograms hematopoiesis via upregulation of Spi1 transcription. Nature Communications. 9, 4239-4250 (2018).

15. M Kurokawa, K Mitani, K Irie, T Matsuyama, T Takahashi, S Chiba, Y Yazaki, K Matsumoto, H Hirai. The oncoprotein Evi-1 represses TGF-beta signaling by inhibiting Smad3. Nature. 394, 92-96 (1998).

16. M Kurokawa, K Mitani, T Yamagata, T Takahashi, K Izutsu, S Ogawa, T Moriguchi, E Nishida, Y Yazaki, H Hirai. The evi-1 oncoprotein inhibits c-Jun N-terminal kinase and prevents stress-induced cell death. EMBO J. 19, 2958-2968 (2000).

17. T Tanaka, J Nishida, K Mitani, S Ogawa, Y Yazaki, H Hirai. Evi-1 raises AP-1 activity and stimulates c-fos promoter transactivation with dependence on the second zinc finger domain. J Biol Chem. 269, 24020-24026 (1994).

18. OS Kustikova, A Schwarzer, M Stahlhut, MH Brugman, T Neumann, M Yang, Z Li, A Schambach, N Heinz, S Gerdes, I Roeder, TC Ha, D Steinmann, B Schiegelberger, and C Baum. Activation of Evi1 inhibits cell cycle progression and differentiation of hematopoietic progenitor cells. Leukemia. 27, 1127-1138 (2013).

19. S Goyama, G Yamamoto, M Shimabe, T Sato, M Ichikawa, S Ogawa, S Chiba, M Kurokawa. Evi-1 is a critical regulator for hematopoietic stem cells and transformed leukemia cells. Cell Stem Cell. 3, 207-220 (2008)

20. OS Kustikova, A Schwarzer, M Stahlhut, MH Brugman, T Neumannn, M Yang, Z Li, A Schambach, N Heinz, S Gerdes, I Roeder, TC Ha, D Steinemann, B Schlegelberger,

and C Baum. Activation of Evi1 inhibits cell cycle progression and differentiation of hematopoietic progenitor cells. Leukemia. 27, 1127-1138 (2013).

21. TA Konrad, A Karger, H Hacki, I Schwarzinger, I Herbaek, R Wieser. Inducible expression of EVI1 in human myeloid cells causes phenotypes consistent with its role in myelodysplastic syndromes. J Neukoc Biol. 86, 813-822 (2009).
22. N Yamakawa, K Kaneda, Y Saito, E Ichihara, K Morishita. The increased expression of integrin alpha6 (ITGA6) enhances drug resistance in EVI1 (high) leukemia. PLOS ONE. 7, e30706 (2012).
23. K Karakaya, E Herbst, C Ball, H Glimm, A Krämer, H Löffer. Overexpression of EVI1 interferes with cytokinesis and leads to accumulation of cells with supernumerary centrosomes in G0/1 phase. Cell Cycle. 11, 3492-3503 (2012).
24. N Fenouille, CF Bassil, I Ben-Sahra, L Benajiba, G Alexe, A Ramos, Y Pikman, AS Conway, MR Burgess, Q Li, F Luciano, P Auberger, I Galinsky, DJ DeAngelo, RM Stone, Y Zhang, AS Perkins, K Shannon, MT Hemann, A Puissant, K Stegmaier. The creatine kinase pathway is a metabolic vulnerability in EVI1-positive acute myeloid leukemia. Nature Medicine. 23, 301-313 (2017).
25. L Benajiba, G Alexe, A Su, E Raffoux, J Soulier, MT Hemann, O Hermine, R Irzykson, K Stegmaier, A Puissant. Creatine kinase pathway inhibition alters GSK3

and WNT signaling in EVI1-positie AML. Leukemia. doi:10.1038/s41375-018-0291-x. [Epub ahead of print] (2018).

26. MV Liverti, JW Locasale. The Warburg Effect: How Does it Benefit Cancer Cells? Trends Biochem Sci 41, 211-218 (2016).

27. Q Li, P Wei, J Wu, M Zhang, G Li, Y Li, Y Xu, X Li, D Xie, S Cai, K Xie, D Li. The FOXC/FBP1 signaling axis promotes colorectal cancer proliferation by enhancing the Warburg effect. Oncogene doi:10.1038/s41388-018-0469-8 [Epub ahead of print] (2018).

28. YH Wang, WJ Israelsen, D Lee, VWC Yu, NT Jeanson, CB Clish, LC Cantley, MG Vnader Heiden, and DT Scadden. Cell-State-Specific Metabolic Dependency in Hematopoiesis and Leukemogenesis. Cell. 158, 1309-1323 (2014).

29. S Furutachi, H Miya, T Watanabe, H Kawai, N Yamasaki, Y Harada, I Imayoshi, M Nelson, K Nakayama, Y Hirabayashi, Y Gotoh. Slowly dividing neural progenitors are an embryonic origin of adult neural stem cells. Nature neuroscience 18, 657-665 (2105).

30. Y Kanda. Investigation of the freely available easy-to-use software ‘EZR’ for medical statistics. . Bone Marrow Transplantation. 48, 452-458 (2013).

31. B Li, B Qiu, DSM Lee, ZE Walton, JD Ochocki, LK Mathew, A Mancuso, TPF Gade, B Keith, I Nissim, MC Simon. Fructose-1, 6-bisphosphatase opposes renal carcinoma progression. Nature. 513, 251-255 (2014).

32. C Dong, T Yuan, Y Wu, Y Wang, TWM Fan, S Miriyaa, Y Lin, J Yao, J Shi, T Kang, P Lorkiewicz, D St Clair, MC Hung, BM Evers, BP Zhou. Loss of FBP1 by Snail-Mediated Repression Provides Metabolic Advantages in Basal-like Breast Cancer. Cancer Cell. 23, 316-331 (2013).

33. H Hirata, K Sugimachi, H Komatsu, M Ueda, T Masuda, R Uchi, S Sakimura, S Nambara, T Saito, Y Shinden, T Iguchi, H Eguchi, S Ito, K Terashima, K Sakamoto, M Hirakawa, H Honda, K Mimori. Decreased Expression of Fructose-1, 6-bisphosphatase Associates with Glucose Metabolism and Tumor Progression in Hepatocellular Carcinoma. Cancer Res. 76, 3265-3276 (2016).

34. TY Li, Y Sun, Y Liang, Q Liu, Y Shi, CS Zhang, C Zhang, L Song, P Zhang, X Zhang, X Li, T Chen, HY Huang, X He, Y Wang, YQ Wu, S Chen, M Jiang, C Chen, C Xie, JY Yang, Y Lin, S Zhao, Z Ye, SY Lin, DTy Chiu, SC Lin. ULK1/2 Constitute a Bifurcate Node Controlling Glucose Metabolic Fluxes in Addition to Autophagy. Molecular Cell. 62, 359-370 (2016).

35. LY Chen, CS Cheng, C Qu, P Wang, H Chen, ZQ Meng, Z Chen. CBX3 promotes proliferation and regulates glycolysis via suppressing FBP1 in pancreatic cancer. Biochem and Biophys Res Commun, 500, 691-697 (2018).

36. GG Loots, I Ovcharenko. rVISTA 2.0: evolutionary analysis of transcription factor binding sites. Nucleic Acids Res. 1, W217-221 (Web Server issue) (2004).

37. H Yuasa, Y Oike, A Iwama, I Nishikata, D Sugiyama, A Perkins, ML Muchenski, T Suda, K Morishita. Oncogenic transcription factor Evi1 regulates hematopoietic stem cell proliferation through GATA-2 expression. EMBO J. 24, 1976-1987 (2005).

38. O Warburg. On the Origin of Cancer Cells. Science. 123, 309-314 (1956).

39. MV Liberti and JW Locasale. The Warburg Effect: How Does it Benefit Cancer Cells? Trends Biochem Sci. 41, 211-218 (2016).

40. E Kavanagh, B Joseph. The hallmarks of CDKN1C (p57, KIP2) in cancer. Biochemica et Biophysica Acta. 1816, 50-96 (2011).

41. S Matsuoka, MC Edwards, C Bai, S Parker, P Zhang, A Baldini, JW Harper, SJ Elledge. p57KIP2, a structurally distinct member of the p21CIP1 Cdk inhibitor family, is a candidate tumor suppressor gene. Gene Dev. 9, 650-662 (1995).

42. D Hanahan, RA Weinberg. The hallmarks of cancer. Cell. 100, 57-70 (2000).

43. RJ Jin, Y Lho, Y Wang, M Ao, MP Revelo, SW Hayward, ML Wills, SK Logan, P Zhang, RJ Matusik. Down-regulation of p57Kip2 induces prostate cancer in the mouse. Cancer Res. 68, 3601-3608 (2008).

44. O Riccio, ME van Gijn, AC Bezdek, L Pellegrinet, JH van Es, U Zimber-Strobl, LJ Strobl, T Honjo, H Clevers, F Radtke. Loss of intestinal crypt progenitor cells owing to inactivation of both Notch1 and Notch2 is accompanied by derepression of CDK inhibitors p27Kip1 and p57Kip2. EMBO Rep. 9, 377-383 (2008).

45. Z Wang, AS Azmi, A Ahmad, S Banerjee, S Wang, FH Sarkar, RM Mohammad. TW-37, a small molecule inhibitor of Bcl-2, inhibits cell growth and induces apoptosis in pancreatic cancer: involvement of Notch-1 signaling pathway. Cancer Res. 69, 2757-2765 (2009).

46. A Radujkovic, S Dietrich, M Andrulis, A Benner, T Longerich, A Pellagatti, K Nanda, T Giese, U Germing, S Baldus, J Boultwood, AD Ho, P Dreger, T Luft. Expression of CDKN1C in the bone marrow of patients with myelodysplastic syndrome and secondary acute myeloid leukemia is associated with poor survival after conventional chemotherapy. Int J Cancer. 139, 1403-1413 (2016).

47. A Borriello, I Caldarelli, D Bencivenga, V Cucciolla, A Liva, E Usala, P Danise, L Ronzoni, S Perrotta, F Della Ragione. p57Kip2 is a downstream effector of BCR-

ABL kinase inhibitors in chronic myelogenous leukemia cells. Carcinogenesis 32, 10-18 (2011).

48. Y Zhang, S Stehling-Sun, K Lezon-Geyda, SC Juneja, L Coillard, G Chatterjee, CA Wuertzer, F Camargo, AS Perkins. PR-domain-containing Mds1-Evi1 is critical for long-term hematopoietic stem cell function. Blood. 118, 3853-3861 (2011).
49. R Ihaka, and R Gentoleman. R: a language for data analysis and graphics. J Comp Graph Stat. 5, 299-314. (1996).
50. T Farge, E Saland, F de Toni, N Aroua, M Hosseini, R Perry, C Bosc, M Sugita, L Stuani, M Fraisse, S Scotland, C Larrue, H Boutzen, V Feliu, ML Nicolau-Travers, S Cassant-Sourdy, N Broin, M David, N Serhan, A Sarry, S Tavitian, T Kaoma, L Vallar, J Iacovoni, LK Linares, C Montersino, R Castellano, E Griessinger, Y Collette, O Duchamp, Y Barreira, P Hirsch, T Palama, L Gales, F Delhommeau, BH Garmy-Susini, JC Portais, F Vergez, M Selak, G Danet-Desnoyers, M Carroll, C Recher, JE Sarry. Chemotherapy-Resistant Human Acute Myeloid Leukemia cells Are Not Enrichment for Leukemia Stem Cells but Require Oxidative Metabolism. Cancer Discovery. 7, 716-735 (2017).

51. C Glass, C Wuertzer, X Cui, Y Bi, R Davuluri, YY Xial, M Wilson, K Owens, Y Zhang, A Perkins. Global Identification of EVI1 Target Genes in Acute Myeloid Leukemia. PLOS ONE. 8, e67134 (2013).

52. IP Pateras, K Apostolopoulou, K Niforou, A Kotsinas, VG Gorgoulis. $p57^{KIP2}$: "Kip"ing the Cell under Control. Mol Cancer Res. 7, 1902-1919 (2009).

53. Y Hashimoto, K Kohri, Y Kaneko, H Morisaki, T Kato, K Ikeda, M Nakanishi. Critical Role for the $3_{10}$ Helix Region of $p57^{KIP2}$ in Cyclin-dependent Kinase 2 Inhiition and Growth Suppression. Journal of Biological Chemistry. 273(26), 16544-16550 (1998).

54. E Cerami, J Gao, U Dogrusoz, BE Gross, SO Sumer, BA Aksoy, A Jacobsen, CJ Byrne, ML Heuer, E Larsson, Y Antipin, B Reva, AP Goldberg, C Sander, N Schultz. The cBio Cancer Genomics Portal: An Open Platform for Exploring Multidimensional Cancer Genomics Data. Cancer Discovery. 2(5), 401-404 (2012).

55. J Gao, BA Aksoy, U Dogrusoz, G Dresdner, B Gross, SO Sumer, Y Sun, A Jacobsen, R Sinha, E Larsson, E Cerami, C Sander, N Schultz. Integrative Analysis of Complex Cancer Genomics and Clinical Profiles Using the cBioPortal. Science Signaling. 6(269), pl1 (2013).

56. GA Challen, N Boles, KK Lin, MA Goodell. Mouse Hematopoietic Stem Cell Identification And Analysis. Cytometry A. 75(1), 14-24 (2009).

57. MH Lee, I Reynisdottir, J Massague. Cloning of $p57^{KIP2}$, a cyclin-dependent kinase inhibitor with unique domain structure and tissue distribution. Genes and Development. 9:639-649 (1995).

58. A Subramanian, P Tamayo, VK Mootha, S Mukherjee, BL Ebert, MA Gilette, A Paulovich, SL Pomeroy, TR Golub, ES Lander, JP Mesirov. Gene set enrichment analysis: A knowledge-based approach for interpreting genome-wide expression profiles. PNAS. 102(43), 15545-15550 (2005).

59. VK Mootha, CM Lindgren, KF Eriksson, A Subramanian, S Sihag, J Lehar, P Puigserver, E Carlsson, M Ridderstrale, E Laurila, N Houstis, MJ Daly, N Patterson, JP Mesirov, TR Golub, P Tamayo, B Spiegelman, ES Lander, JN Hirschhorn, D Altschuler, LC Groop. PGC-1 $\alpha$ -responsive genes involved in oxidative phosphorylation are coordinately downregulated in human diabetes. Nature genetics. 34, 267-273 (2003).

60. TW von Geldern, C Lai, RJ Gum, M Daly, C Sun, EH Fry, C Abad-Zapatero. Benzoxazole benzenesulfonamides are novel allosteric inhibitors of fructose-1,6-

bisphophatase with a distinct binding mode. Bioorganic and Medicinal Chemistry Letters. 16, 1811-1815 (2006).

61. Q Dang, SR Kasibhatla, W Xiao, Y Liu, J DaRe, F Taplin, KR Reddy, GR Scarlato, T Gibson, PD van Poelje, SC Potter, MD Erion. Fructose-1,6-phosphatase Inhibitors. 2. Design, Synthesis, and Structure – Activity Relationship of a Series of Phosphonic Acid Containing Benzimidazoles that Function as 5'-Adenosinemonophosphate (AMP) Mimics. Journal of Medicinal Chemistry. 53, 441-451 (2010).

62. CL Jones, BM Stevens, A D'Alessandro, JA Reisz, R Culp-Hill, T Nemkov, S Pei, N Khan, B Adane, H Ye, A Krug, D Reinhold, C Smith, J DeGregori, DA Pollyea, CT Jordan. Inhibition of Amino Acid Metabolism Selectivity Targets Human Leukemia Stem Cells. Cancer Cell. 34, 724-740 (2018).